

# Bridging Supervised and Temporal Difference Learning with $Q$ -Conditioned Maximization

Xing Lei<sup>1</sup>   Zifeng Zhuang<sup>2</sup>   Shentao Yang<sup>3</sup>   Sheng Xu<sup>4</sup>   Yunhao Luo<sup>5</sup>

Fei Shen<sup>6</sup>   Xuetao Zhang<sup>1,†</sup>   Donglin Wang<sup>2,†</sup>

<sup>1</sup>Xi'an Jiaotong University   <sup>2</sup>Westlake University   <sup>3</sup>University of Texas at Austin  
<sup>4</sup>The Chinese University of Hong Kong, Shenzhen  
<sup>5</sup>Georgia Institute of Technology   <sup>6</sup>National University of Singapore  
leixing@stu.xjtu.edu.cn

## Abstract

Recently, supervised learning (SL) methodology has emerged as an effective approach for offline reinforcement learning (RL) due to their simplicity, stability, and efficiency. However, recent studies show that SL methods lack the trajectory stitching capability, typically associated with temporal difference (TD)-based approaches. A question naturally surfaces: *How can we endow SL methods with stitching capability and bridge its performance gap with TD learning?* To answer this question, we introduce  $Q$ -conditioned maximization supervised learning for offline goal-conditioned RL, which enhances SL with the stitching capability through  $Q$ -conditioned policy and  $Q$ -conditioned maximization. Concretely, we propose **Goal-Conditioned Reinforced Supervised Learning (GCR<sub>SL</sub>)**, which consists of (1) estimating the  $Q$ -function by CVAE from the offline dataset and (2) finding the maximum  $Q$ -value within the data support by integrating  $Q$ -function maximization with Expectile Regression. In inference time, our policy chooses optimal actions based on such a maximum  $Q$ -value. Experimental results from stitching evaluations on offline RL datasets demonstrate that our method outperforms prior SL approaches with stitching capabilities and goal data augmentation techniques.

## 1 Introduction

Several recent papers reframes reinforcement learning (RL) as a pure supervised learning (SL) problem [Schmidhuber, 2020, Chen et al., 2021, Emmons et al., 2021, Ghosh et al., 2021], which has gained attention due to its simplicity, stability and scalability [Lee et al., 2022a]. They typically assign labels to state-action pairs in the offline dataset based on the derived future outcomes (e.g., achieving a goal [Ghosh et al., 2021] or a return [Chen et al., 2021]); then maximize the likelihood of these actions by treating them as optimal for producing the labeled outcomes. These approaches, termed as outcome-conditioned behavioral cloning (OCBC), have demonstrated excellent results in offline RL [Fu et al., 2020, Emmons et al., 2021]. Nevertheless, recent studies [Yang et al., 2023b, Ghugare et al., 2024] has identified these SL methods as the lack of stitching capability [Ziebart et al., 2008]. This is primarily because they do not maximize the  $Q$ -value [Kim et al., 2024]. In contrast, temporal difference (TD)-based RL methods (e.g., CQL [Kumar et al., 2020], IQL [Kostrikov et al.,

<sup>†</sup> Corresponding Author.

2021)) possess stitching capability by learning and maximizing a  $Q$ -function, though they frequently encounter instability and optimization challenges [Van Hasselt et al., 2018, Kumar et al., 2019] due to bootstrapping and projection into a parameterized policy space while maximizing the  $Q$ -value.

To get the benefit of both world, in this paper, we focus on enhancing the stitching capability of SL-based method in offline RL while maintaining OCBC’s stability. Inspired by recent max-return sequence modeling [Zhuang et al., 2024], we propose a  $Q$ -conditioned maximization supervised learning framework. We aim to incorporate  $Q$ -value as a conditioning factor in OCBC to acquire stitching capability, using the predicted maximum *in-distribution* [Kostrikov et al., 2021]  $Q$ -value to determine the optimal action during inference, where the  $Q$ -value is supported by the offline dataset and is estimated via expectile regression [Aigner et al., 1976, Sobotka and Kneib, 2012].

Algorithmically, we present **Goal-Conditioned Reinforced Supervised Learning (GCREinSL)**, which implements  $Q$ -conditioned maximization supervised learning for OCBC methods, instantiated via DT [Chen et al., 2021] and RvS [Emmons et al., 2021]. **GCREinSL** first estimates the  $Q$ -value from the offline dataset using a CVAE [Sohn et al., 2015], and subsequently estimate the maximum  $Q$ -value together with the OCBC policy training. This two-stage pipeline remove the need for the unstable bootstrapping in standard TD-based method in learning the optimal  $Q$ -value. **GCREinSL** not only learns the mapping between  $Q$ -value and action in the dataset, but also estimates the highest attainable *in-distribution*  $Q$ -value during inference.

Despite its simplicity, the effectiveness of **GCREinSL** is empirically demonstrated on offline goal-conditioned RL datasets that require stitching Ghugare et al. [2024], outperforming prior OCBC methods and goal data augmentation methods [Yang et al., 2023b, Ghugare et al., 2024]. Furthermore, we extend our approach to return-conditioned RL without an explicit goal state, and compare it with state-of-the-art (SOTA) sequence modeling RL methods. Results on D4RL Antmaze [Fu et al., 2020] datasets show that our method continues to outperform related methods that also perform stitching. Theoretical and experimental evidence further indicates that our **GCREinSL** effectively closes the gap between OCBC and TD-based methods.

## 2 Related Work

**Offline Goal-conditioned RL.** This paper focuses on offline goal-conditioned RL. Previous studies have widely explored this topic using various methodologies. Representative approaches include goal-conditioned hindsight relabeling [Andrychowicz et al., 2017], hierarchical learning [Chane-Sane et al., 2021, Li et al., 2022, Park et al., 2023], planning [Lee et al., 2022b, Kim et al., 2023, Yoon et al., 2024, Wang et al., 2024a, Eysenbach et al., 2025, Luo et al., 2025], metric learning [Wang et al., 2023, Park et al., 2024, Myers et al., 2024], dual optimization [Ma et al., 2022, 2023, Sikchi et al., 2024], generative modeling [Zeng et al., 2023, Hong et al., 2023, Reuss et al., 2023, Jain and Ravanbakhsh, 2024] have been employed to learn goal-conditioned policies. These methods have demonstrated success across diverse tasks, including real-world robotic systems [Shah et al., 2022, Zheng et al., 2023, Park et al., 2025]. As aforementioned TD-based methods often encounters instability and inefficiencies in optimization [Van Hasselt et al., 2018, Kumar et al., 2019, Ghosh et al., 2021], therefore we focus on the simple yet efficient OCBC methods [Ding et al., 2019, Schmidhuber, 2020, Lynch et al., 2020, Chen et al., 2021, Ghosh et al., 2021, Emmons et al., 2021, Yang et al., 2022, 2023a, Hejna et al., 2023]. Furthermore, unlike previous techniques that depend on manually defined reward or distance functions, our approach treating the goal-conditioned RL task as one of predicting future state visitation [Eysenbach et al., 2020, 2022b, Zheng et al., 2024, Ghugare et al., 2024, Borkiewicz et al., 2025].

**Enhancing SL with Stitching Capability.** The concept of trajectory stitching, as discussed by Ziebart et al. [2008], is a characteristic property of TD-learning methods [Kumar et al., 2020, Kostrikov et al., 2021], which employ dynamic programming. This property enables these methods to integrate data from diverse trajectories, thereby improving their ability to handle complex tasks by effectively utilizing available data [Cheikhi and Russo, 2023]. On the other hand, most SL-based methods, such as DT [Chen et al., 2021] and RvS [Emmons et al., 2021], lack this capability. Brandfonbrener et al. [2022], Yang et al. [2023b] provide extensive experiments where SL algorithms do not perform stitching and Ghugare et al. [2024] also demonstrates this from the perspective of combinatorial generalisation. Then they propose goal data augmentation for SL, yet these methods may struggle with correctly selecting augmented goal, such as unreachable goals [Yang et al., 2023b]. Unlike these

methods, we first present an illustrative example to demonstrate that the SL approach lacks stitching capability. Subsequently, we enhance the stitching ability of SL by embedding the goal-reaching probability from the goal-conditioned RL objective and maximizing it. We also observe that several recent supervised learning methods [Jiang et al., 2023, Zeng et al., 2023, Kim et al., 2024] exhibit competitive stitching properties; however, in contrast to these approaches, our method does not depend on model-based mechanisms or dynamic programming. Conversely, other supervised learning methods, akin to our framework [Yamagata et al., 2023, Wu et al., 2023, Zhuang et al., 2024, Wang et al., 2024b], have made like one-step RL [Brandfonbrener et al., 2021, Zhuang et al., 2023] in enabling OCBC to demonstrate stitching properties; nevertheless, their capability remains constrained. Our **GCreinSL** significantly addresses this limitation.

### 3 Preliminaries

#### 3.1 Goal-conditioned RL in Controlled Markov Process

We study the problem of goal-conditioned RL in a controlled Markov process with states  $s \in \mathcal{S}$ , actions  $a \in \mathcal{A}$ . The dynamics is  $p(s' | s, a)$ , the initial state distribution is  $p_0(s_0)$ , the discount factor is  $\gamma$ , and a reward function  $r(s, a, g)$  for each goal. The goal-conditioned policy  $\pi(a | s, g)$  is conditioned on a pair of state and goal  $s, g \in \mathcal{S} \times \mathcal{G}$ .

For a policy  $\pi$ , we denote the  $t$ -step state distribution  $p_t^\pi(s_t | s_0, a_0)$  as the distribution of states  $t$  steps in the future given the initial state  $s_0$  and action  $a_0$ . We can then define the discounted state occupancy distribution as:

$$p_+^\pi(s_{t+} | s, a) \triangleq (1 - \gamma) \sum_{t=0}^{\infty} \gamma^t p_t^\pi(s_{t+} | s, a), \quad (1)$$

where  $s_{t+}$  is the dummy variable that specifies a future state corresponding to the discounted state occupancy distribution. For a given distribution over goals  $g \sim p_G(g)$ , the objective of the policy  $\pi$  is to maximize the probability of reaching the goal  $g$  in the future:

$$\max_{\pi(\cdot | \cdot, \cdot)} \mathbb{E}_{p_0(s_0) p_G(g) \pi(a_0 | s_0, g)} [p_+^\pi(g | s_0, a_0)]. \quad (2)$$

Following prior work [Eysenbach et al., 2020, Chane-Sane et al., 2021, Blier et al., 2021, Rudner et al., 2021, Eysenbach et al., 2022b, Borkiewicz et al., 2025], we define the goal-conditioned reward function  $r(s, a, g)$  for each goal as the probability of reaching the goal at the next time step:

$$r(s_t, a_t, g) \triangleq (1 - \gamma) \gamma p(s_{t+1} = g | s_t, a_t). \quad (3)$$

And the corresponding  $Q$ -function for a policy  $\pi(\cdot | \cdot, g)$  can be defined as

$$Q^\pi(s, a, g) \triangleq \mathbb{E}_{\pi(\cdot | \cdot, g)} \left[ \sum_{t=0}^{\infty} \gamma^t r(s_t, a_t, g) \mid \begin{smallmatrix} s_0=s, \\ a_0=a \end{smallmatrix} \right]. \quad (4)$$

**Offline Setting.** Our work focuses on the offline RL setting [Levine et al., 2020], the agent can only access a static offline dataset  $\mathcal{D}$  and cannot interact with the environment. The offline dataset  $\mathcal{D}$  can be collected from an unknown behavior policy  $\beta$  [Levine et al., 2020, Prudencio et al., 2023]. We can express the offline dataset as  $\mathcal{D} := \{\tau_i\}_{i=1}^N$  [Ghugare et al., 2024], where  $\tau_i := \{ \langle s_0^i, \eta_0^i, a_0^i, r_0^i \rangle, \langle s_1^i, \eta_1^i, a_1^i, r_1^i \rangle, \dots, \langle s_T^i, \eta_T^i, a_T^i, r_T^i \rangle, g^i \}$  is the goal-conditioned trajectory and  $N$  is the number of stored trajectories. In each  $\tau_i$ ,  $s_0^i \sim p_0(s_0)$ , and  $\eta$  is the state’s corresponding representation in the goal space calculated using  $\eta_t = \phi(s_t^i)$ , where  $\phi : \mathcal{S} \rightarrow \mathcal{G}$  is a known state-to-goal mapping. The desired goal  $g^i$  is randomly sampled from  $p(g)$ . It should be noted that trajectories may be unsuccessful (i.e.,  $\eta_T^i \neq g^i$ ). Goal-conditioned methods often utilize  $\eta_t, 0 \leq t \leq T$  as relabeled goals  $g$  for training.

#### 3.2 Outcome Conditional Behavioral Cloning (OCBC)

We adopt a simple and popular class of goal-conditioned RL methods: outcome conditioned behavioral cloning [Eysenbach et al., 2022a], which encompasses DT [Chen et al., 2021], URL [Schmidhuber, 2020], RvS [Emmons et al., 2021], GCSL [Ghosh et al., 2021] and so on. These SL methods take as input the offline dataset  $\mathcal{D}$  and learn a goal-conditioned policy  $\pi(a | s, g)$  using a maximum likelihood objective:

$$\max_{\pi(\cdot | \cdot, \cdot)} \mathbb{E}_{(s, a, g) \sim \mathcal{D}} [\log \pi(a | s, g)]. \quad (5)$$

## 4 Stitching in OCBC: Goal-reaching Probability-conditioned Maximization

In the offline RL literature, trajectory stitching has garnered significant attention. Recent research by Ghugare et al. [2024] interprets stitching from the perspective of combinatorial generalisation and demonstrates that OCBC methods lack the effective stitching capabilities. This finding is also corroborated experimentally by Yang et al. [2023b]. Then they propose goal data augmentation methods that enhances the stitching performance of OCBC. Motivated by these prior works, we illustrate the limitations of OCBC in achieving stitching capability; however, unlike previous studies, we enable OCBC to acquire this capability by conditioning on the maximized goal-reaching probability.

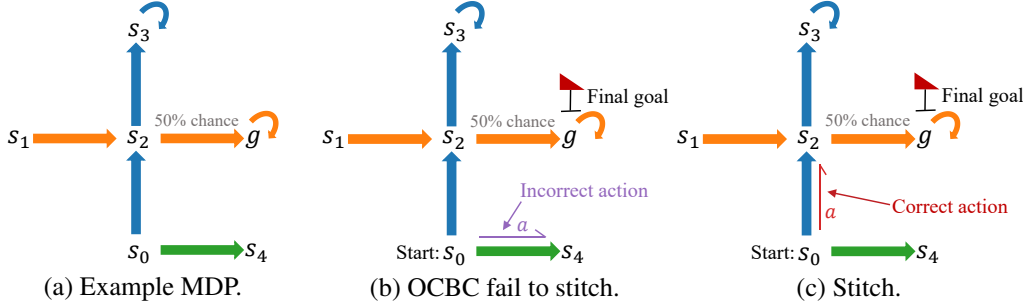


Figure 1: An illustrative example for stitching analysis. (a) **Example MDP**: The MDP has five states, one goal and two actions (up  $\uparrow$  and right  $\rightarrow$ ). One example offline dataset  $\mathcal{D}_{\text{MDP}}$  contains two trajectories  $\tau_1 = \{s_0, s_2, s_3\}$  and  $\tau_2 = \{s_1, s_2, g\}$ , distinguished by blue and orange. Another green trajectory  $\tau_3 = \{s_0, s_4\}$  is not in  $\mathcal{D}_{\text{MDP}}$ . (b) **OCBC fails to stitch**: Given the start state  $s_0$  and the final goal  $g$ , the classical OCBC policy tends to take the incorrect action (right,  $a \rightarrow$ ) that leads to undesired goal state  $s_4$ . (c) **GCreinSL succeeds to stitch**: In contrast, given the  $s_0$  and  $g$ , the **GCreinSL** policy is able to take the correct action (up,  $a \uparrow$ ), causing  $s_0 \rightarrow s_2 \rightarrow g$ .

To demonstrate the lack of trajectory stitching in OCBC methods, consider the example in Figure 1:  $s_0$  is the starting state,  $g$  is the final goal. The example offline data  $\mathcal{D}$  contains two trajectories  $\tau_1 = \{s_0, s_2, s_3\}$  and  $\tau_2 = \{s_1, s_2, g\}$ . During inference, we expect that the policy can achieve the final goal  $g$  given the start  $s_0$ . However, no trajectory in  $\mathcal{D}$  goes directly from start  $s_0$  to final goal  $g$ . In this case, starting from start  $s_0$  and conditioned on  $g$ , the SL-based OCBC policy tends to take the wrong right action  $\rightarrow$  because the policy believes the up action  $\uparrow$  will achieve the state  $s_3$  rather than  $g$  due the existence of the blue trajectory  $\tau_1$ .

Ideally, the policy should stitch the existing trajectories and take one **stitched** trajectory  $\tau^* = \{s_0, s_2, g\}$  to achieve  $g$  from start  $s_0$ . Dynamic programming based methods can propagate rewards through the backwards **stitch** path of  $g \rightarrow s_2 \rightarrow s_0$  to output the correct action. Therefore, Yang et al. [2023b], Ghugare et al. [2024] propose an additional sampling of trajectory  $\{s_0, g\}$  during the OCBC training phase and describe their approach as goal data augmentation. In contrast, we additionally introduce a probability-conditioned policy, namely  $\pi(a|s, g, P)$ . And during the inference phase, one proper probability  $P^*$  is adopted to make this policy take the correct action.

To select a proper  $P^*$ , first, we denote  $P(s, a, g)$  as the probability of reaching goal  $g$  in the future by taking action  $a$  from state  $s$  (consistent with the probability definition in Equation (2)), it is evident that the following holds:  $P(s_0, a \uparrow, g) = 1/2$ , and  $P(s_0, a \rightarrow, g) = 0$ . When policy aims to achieve the final goal  $g$  given the start  $s_0$ , we can use extra  $P$  condition to guide the policy. Concretely, given the maximized conditional  $P^* = \max[P(s_0, a \uparrow, g), P(s_0, a \rightarrow, g)] = 1/2$ , the P-conditioned policy  $\pi(\cdot|s_0, g, P^*)$  will take the up action  $\uparrow$  to achieve the desired goal-reaching probability.

## 5 GCreinSL: Goal-Conditioned Reinforced Supervised Learning

From the perspective outlined in Section 4, we aim to equip OCBC methods with the ability to maximize the expected probability of reaching the goal, as described in Equation (2). Recalling that the goal-reaching probability is equivalent to  $Q$ -function in GCRL (Section 5.1), in Section 5.2, we introduce the framework of  $Q$ -conditioned maximization supervised learning and theoretically demonstrate that this paradigm can achieve maximum  $Q$ -value without encountering the out-of-distribution (OOD) issue. In Section 5.3, we outline the practice implementation of our **GCreinSL**.



## 5.1 The Relationship Between Goal-reaching Probability and $Q$ -function

**Theorem 5.1** (Rephrased from Proposition 1 of Eysenbach et al. [2022b] : probabilities  $\rightarrow$  rewards). *The probability of reaching goal  $g$  under the discounted state occupancy measure in Equation (1) is equivalent to the  $Q$ -function for the goal-conditioned reward function in Equation (4):*

$$p_+^\pi(s_{t+} = g \mid s, a) = Q^\pi(s, a, g). \quad (6)$$

This theorem indicates that under the definition of reward in Equation (3), the goal-reaching probability  $p_+^\pi(s_{t+} = g \mid s, a)$  is equivalent to a  $Q$ -function  $Q^\pi(s, a, g)$ .

Translating probability into reward simplifies the analysis of goal-conditioned RL and enables the use of probabilistic model, such as CVAE [Sohn et al., 2015], for  $Q$ -function estimation. In Section 5.3.1, we provide the detailed implementation for estimating the goal-reaching probability/ $Q$ -function using CVAE.

## 5.2 $Q$ -conditioned maximization supervised learning

Assume that we can accurately estimate the  $Q$ -function  $Q^\beta(s, a, g)$  of the behavior policy  $\beta$  for each state-action pair in the offline dataset (i.e., accurately obtain the goal-reaching probability for a given goal along the same trajectory), we aim to equip supervised learning with an additional objective of maximizing  $Q$ -function so as to obtain the maximum *in-distribution*  $Q$ -value. Then, during inference, the policy can select (near-) optimal action conditioned on the *in-distribution* maximized  $Q$ -value. Expectile regression [Newey and Powell, 1987] is suitable to capture the upper distribution bound [Kostrikov et al., 2021, Wu et al., 2023, Zhuang et al., 2024], so we employ it as  $Q$ -function loss for estimating the maximum *in-distribution*  $Q$ -value.

Specifically, the  $Q$ -function loss based on the expectile regression is as follows:

$$\mathcal{L}_Q^m = \mathbb{E}_{(s,a,g) \sim \mathcal{D}} [ |m - \mathbb{1}(\Delta Q < 0)| \Delta Q^2 ], \quad (7)$$

here  $\Delta Q = Q^\beta - \hat{Q}$  and  $\hat{Q}$  is the predicted  $Q$ -value for the learned policy  $\pi$  that can come from the supervised learning model (e.g., DT model can independently predict both the  $Q$ -value and the corresponding actions). Here  $m \in (0, 1)$  is the hyperparameter of expectile regression. When  $m = 0.5$ , expectile regression reduces to the standard Mean Squared Error (MSE) loss. However, when  $m > 0.5$ , this asymmetric loss function places greater weight on  $Q$ -values larger than  $\hat{Q}$ . In other words, the predicted  $Q$ -value  $\hat{Q}(s, a)$  will approach larger  $Q^\beta(s, a)$ .

To reveal what the  $Q$ -function loss in Equation (7) will learn and provide a formal explanation of its role, we present the following theorem:

**Theorem 5.2.** *Define  $\mathbf{SG} \doteq (s, g, a, Q^\beta)$ . For  $m \in (0, 1)$ , denote  $\mathbf{Q}^m(\mathbf{SG}) = \arg \min_{\hat{Q}} \mathcal{L}_Q^m(\mathbf{SG})$ , we have*

$$\lim_{m \rightarrow 1} \mathbf{Q}^m(\mathbf{SG}) = Q_{\max}, \forall s, g,$$

where  $Q_{\max} = \max_{\mathbf{a} \sim \mathcal{D}} Q^\beta(s, a, g)$  denotes the maximum  $Q$ -value over all actions under  $s$  in the offline dataset.

The proof is in Appendix A. It is crucial to note that  $Q_{\max}$  here refers to the maximum action value in the dataset, *not the global maximum*, as the offline dataset may not contain the global maximum. Theorem 5.2 indicates the loss  $\mathcal{L}_Q^m$  will make  $\hat{Q}$  predict the maximum  $Q$ -value when  $m \rightarrow 1$ , which is similar to the objective of maximizing the  $Q$ -function in traditional RL.

## 5.3 Practical Implementation

Now, we will focus on the concrete implementation of **GCReinSL**, including the component of goal-reaching probability/ $Q$ -function estimation and the requirement of estimating the maximum  $Q$ -value. The overall structure of **GCReinSL** is depicted in Figure 2.

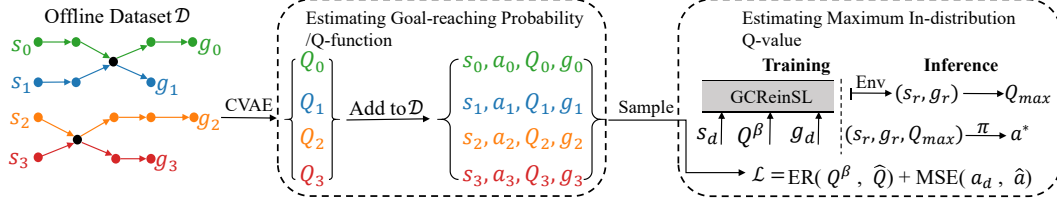


Figure 2: The overview of **GCREinSL** structure.  $[s_0, s_1, s_2, s_3] \in s_d$ ,  $[a_0, a_1, a_2, a_3] \in a_d$ ,  $[g_0, g_1, g_2, g_3] \in g_d$  and  $[Q_0, Q_1, Q_2, Q_3] \in Q^\beta$  come from offline data  $\mathcal{D}$ .  $(s_r, g_r)$  come from environment. ER denotes Expectile Regression.  $Q_{max}$  denotes *in-distribution* max  $Q$ -value.  $\hat{Q}$  and  $\hat{a}$  represent the predicted  $Q$ -value and the output action of the model, respectively. **Left:** The original offline dataset  $\mathcal{D}$ . **Middle:** CVAE as an estimator for the goal-reaching probability/ $Q$ -function. **Right:** The **GCREinSL** model trains using the modified loss  $\mathcal{L}$  and estimates the maximum  $Q$ -value during the inference phase to output the optimal action. Note that our policy here is a  $Q$ -conditioned policy  $\pi(a|s, g, Q)$ , which aligns with the definition provided in Section 4.

### 5.3.1 Estimating goal-reaching probability/ $Q$ -function

The central aim of goal-conditioned RL is to identify the best action for a given state and goal to maximize the chance of reaching the given goal. To achieve this, the first requirement of our method necessitates a precise estimation of the  $Q$ -function  $Q^\beta(s, a, g)$  under the goals appeared in the dataset. Drawing on previous research [Wu et al., 2022, Liu et al., 2024b] and Theorem 5.1, we use CVAE for estimating the goal-reaching probability/ $Q$ -function. Figure 3 succinctly illustrates this process.

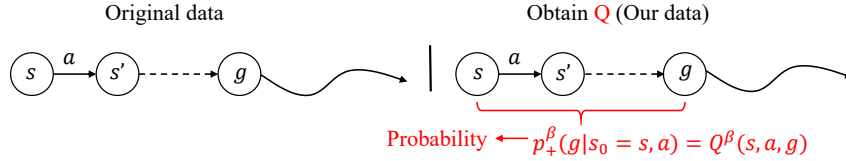


Figure 3: Estimating the  $Q$ -function of the behavior policy via CVAE. **Left:** Original offline trajectory, where the goal  $g$  is reachable from the state  $s$ . **Right:** CVAE is trained by maximizing the lower bound of the log-likelihood  $\log p_+^\beta(g | s_0 = s, a)$ . Note that  $p_+^\beta(g | s_0 = s, a)$  is exactly the goal-reaching probability for the behavior policy  $\beta$ .

**Training (CVAE Pretrain).** In our framework, the probability  $p_+^\beta(g | s_0 = s, a)$  is modeled by a Deep Latent Variable Model, expressed as  $p_\psi(g|s, a) = \int p_\psi(g|z, s, a)p(z|s, a)dz$ , with a prior distribution  $p(z|s, a) = \mathcal{N}(\mathbf{0}, I)$ . Although directly calculating the marginal likelihood  $p_\psi(g|s, a)$  is computationally infeasible, CVAE utilizes an approximate posterior  $q_\varphi(z|s, a, g) \approx p_\psi(z|s, a, g)$ , enabling joint optimization of  $\psi$  and  $\varphi$  parameters via the evidence lower bound (ELBO):

$$\log p_\psi(g|s, a) \geq \mathbb{E}_{q_\varphi(z|s, a, g)} [\log p_\psi(g|z, s, a)] - \text{KL} [q_\varphi(z|s, a, g) \| p(z|s, a)] \stackrel{\text{def}}{=} -\mathcal{L}_{\text{ELBO}}(s, a; \varphi, \psi). \quad (8)$$

**Inference (Probability Estimator).** After training this CVAE, we can approximate the probability  $p_+^\beta(g | s, a)$  in Equation (6) by  $-\mathcal{L}_{\text{ELBO}}$ . To obtain an estimation with lower bias against  $\log p_\psi(g|s, a)$  and hence  $p_+^\beta(g | s, a)$  in Equation (6), we use importance sampling motivated by Rezende et al. [2014], Kingma and Welling [2019], Wu et al. [2022], Liu et al. [2024b]:

$$\begin{aligned} \log p_\psi(g|s, a) &= \log \mathbb{E}_{q_\varphi(z|s, a, g)} \left[ \frac{p_\psi(g, z|s, a)}{q_\varphi(z|s, a, g)} \right] \approx \mathbb{E}_{z^{(l)} \sim q_\varphi(z|s, a, g)} \left[ \log \frac{1}{L} \sum_{l=1}^L \frac{p_\psi(a, g, z^{(l)}|s)}{q_\varphi(z^{(l)}|s, a, g)} \right] \\ &\stackrel{\text{def}}{=} \widehat{\log p_+^\beta(g|s, a; \varphi, \psi, L)}. \end{aligned} \quad (9)$$

From the connection between probability and reward in Theorem 5.1,  $Q^\beta(s, a, g)$  can be derived. In Appendix G.3, we discuss the accuracy of the CVAE in estimating this  $Q^\beta(s, a, g)$ .

### 5.3.2 Estimating the maximum $Q$ -value

After estimating the  $Q$ -value using CVAE, we apply our **GCREinSL** loss for the OCBC to estimate the maximum values within the dataset. The  $Q^\beta(s, a, g)$  values serve as additional conditioning factors in our policy during the training phase. Meanwhile, the estimated maximum  $Q$ -value is used as an additional conditioning factor during inference.

**Training (Integrating the expectile regression into the OCBC loss).** Since our overall agent predicts both  $Q$ -value  $\hat{Q}$  and action  $\hat{a}$ , its training loss consists of a  $Q$ -function loss (Equation (7)) and an action loss. For the action loss, we adopt the MSE loss function in OCBC. We use the same weight for these two loss function terms and therefore the total loss is:

$$\mathcal{L}_{\pi, \hat{Q}}^{\text{GCREinSL}} = \mathbb{E}_{(s, a, g, Q^\beta) \sim \mathcal{D}} \left[ \underbrace{\|a - \pi(s, g, \hat{Q})\|_2^2}_{\text{OCBC}} + \underbrace{|m - \mathbb{1}(\Delta Q < 0)| \Delta Q^2}_{\text{in-distribution max } Q\text{-value}} \right], \quad (10)$$

where  $\Delta Q = Q^\beta - \hat{Q}$  and  $m > 0.5$  represents the hyperparameter of expectile regression.

**Inference (Stitch).** In classical  $Q$ -learning [Mnih et al., 2015], the optimal value function  $Q^*$  can derive the optimal action  $a^*$  given the current state. In the context of OCBC, we are therefore motivated to believe that the maximum  $Q$ -value can help the policy select the (near-)optimal actions. Note that the maximum  $Q$ -value in the offline dataset depends only on the state and goal, as action is “reduced” by the max operation. The inference pipeline of the **GCREinSL** is summarized as follows:

$$\xrightarrow{\text{Env}} (s_0, g_0) \rightarrow \hat{Q}_0 \xrightarrow{\pi} a_0 \xrightarrow{\text{Env}} (s_1, g_1) \rightarrow \hat{Q}_1 \xrightarrow{\pi} a_1 \rightarrow \dots \quad (11)$$

Specially, the environment initializes the state-goal pair  $(s_0, g_0)$  and then our model predicts the maximum  $Q$ -value  $\hat{Q}_0$  given current state-goal pair  $(s_0, g_0)$ . Based on  $\hat{Q}_0$  and  $(s_0, g_0)$ ,  $\pi_\theta$  selects an action  $a_0$ . It is important to note that during inference time, the pair of initial state and goal from the environment may corresponding to the initial state and goal of different trajectories in the offline dataset (like  $\{s_0, g\}$  in Section 4). In this case, our model can still output good actions by stitching together sub-trajectories from multiple trajectories in the dataset. With  $a_0$ , the environment transitions to the next state  $s_1$  and receive the new goal  $g_1$ . In Appendix C, we present the model and algorithm details using DT [Chen et al., 2021] and RvS [Emmons et al., 2021] as the SL backbone.

### 5.4 Comparison and Analysis

To further clarify the differences between OCBC and our **GCREinSL**, as well as the benefits of our changes, we provide a comparison of OCBC and **GCREinSL** in Figure 4. We can observe that our **GCREinSL** introduces an additional conditioning factor,  $Q^\beta$ , and employs expectile regression loss to obtained the maximized *in-distribution*  $Q$ -value  $Q_{max}$ . The inference process determines the optimal action  $a^*$  by considering both the given state-goal pair  $(s_r, g_r)$  and the model predicted  $Q_{max}$ . Note that the learned policy change from  $\pi_O = \pi(a|s, g)$  in OCBC to  $\pi_G = \pi(a|s, g, Q)$  in **GCREinSL**.

Thanks to the additional conditioning on  $Q^\beta$  and the maximization of  $Q_{max}$ , we can incorporate information from other trajectories to facilitate the stitching process. As shown in Figure 1, the agent can select the optimal action by maximizing the  $Q$ -value. Furthermore, our method does not require the unstable bootstrapping in learning the maximum  $Q$ -value, unlike TD-based method such as IQL [Kostrikov et al., 2021], which needs to first learn a  $Q^\beta$  before learning  $\hat{Q}$ . As an extra benefit over the TD-based method, the SL nature of our method removes the need for additional mechanisms to project the  $Q$ -maximizing policy to a parameterized policy space from which one can easily sample, such as CQL [Kumar et al., 2020], TD3+BC [Fujimoto and Gu, 2021] and IQL [Kostrikov et al., 2021]. In Appendix B, we discuss the extension of **GCREinSL** to return-conditioned RL, where there is no concrete goal state.

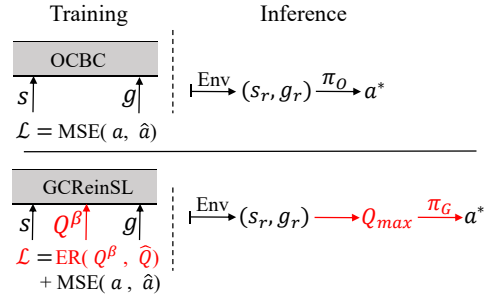


Figure 4: **Left and Right at the Top: OCBC. Left and Right at the Bottom: GCREinSL.**  $s, g$  and  $Q^\beta$  are come from offline data  $\mathcal{D}$ .  $s_r$  and  $g_r$  are come from environment. ER denotes Expectile Regression. The red section highlights the differences.

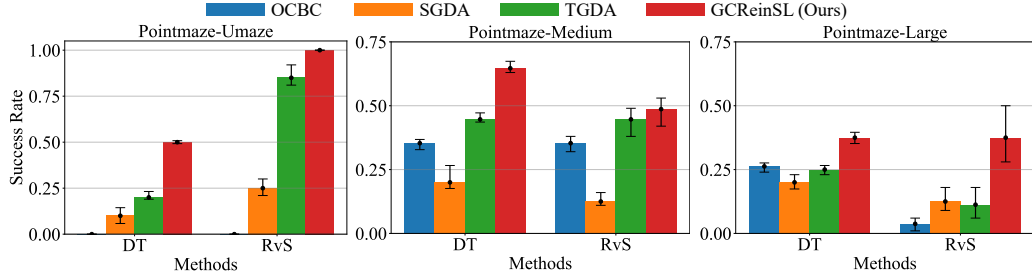


Figure 5: Performance of the original OCBC, as well as OCBC with corresponding goal data augmentation, compared to our SL method **GCREinSL** on the Pointmaze datasets from Ghugare et al. [2024]. Error bars denote 95% bootstrap confidence intervals. **GCREinSL** not only improves the performance of DT and RvS in all tasks, but also outperforms exist goal data augmentation methods.

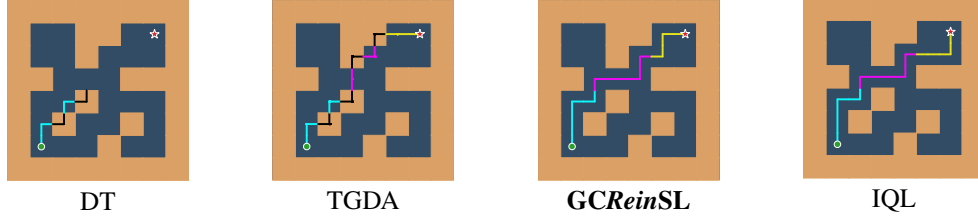


Figure 6: Qualitative Comparison of DT, TGDA, **GCREinSL** for DT and IQL on Ghugare et al. [2024] Pointmaze-Medium task. We observe that DT is unable to reach the specified goal (upper right) from start state (bottom left) and lacks stitching capability. Although TGDA can reach the specified goal, it frequently generates trajectories that cross walls, as it tends to prioritize OOD goals. In contrast, our **GCREinSL** address this issue, and the degree of stitching is comparable to that of IQL.

## 6 Experiments

This section aims to address three key questions: 1) How do the stitching capabilities and degree of stitching of **GCREinSL** perform across different benchmarks? 2) How does **GCREinSL** behave under high-dimensional inputs? 3) When extended to return-conditioned RL, how does it compare to prior sequence modeling methods, and does it narrow the performance gap with TD-based methods?

### 6.1 Experimental Setup

To evaluate the stitching capability of **GCREinSL**, we employ the offline Ghugare et al. [2024] datasets for goal-conditioned RL and D4RL [Fu et al., 2020] Antmaze-v2 datasets for return-conditioned RL. We select RvS [Emmons et al., 2021] and DT [Chen et al., 2021], two competitive methods in OCBC, as baseline models for comparison. We compare **GCREinSL** with three categories of existing methods: (1) for goal data augmentation methods, we include Swapped Goal Data Augmentation (SGDA) [Yang et al., 2023b] and Temporal Goal Data Augmentation (TGDA) [Ghugare et al., 2024] with DT and RvS; for sequence modeling methods, we include Elastic Decision Transformer (EDT) [Wu et al., 2023], Critic-Guided Decision Transformer (CGDT) [Wang et al., 2024b] and Max-Return Sequence Modeling (Reinformer) [Zhuang et al., 2024]; for TD-based RL methods, we include CQL [Kumar et al., 2020] and IQL [Kostrikov et al., 2021]. See Appendix D for more details of baselines. All experiments are conducted using five random seeds. Following the related original paper [Ghugare et al., 2024, Zhuang et al., 2024], we report the final mean success rate in goal-conditioned RL and the best score in return-conditioned RL experiments. Detailed implementations and hyperparameters are provided in Appendix E and Appendix F, respectively.

### 6.2 Testing the Stitching Capability of GCREinSL in Pointmaze Datasets

As shown in Figure 5, it is evident that DT and RvS are struggle to possess stitching property, particularly in the Pointmaze-Umaze and Pointmaze-Large tasks, where their performance is notably poor. However, when  $Q$ -conditioned maximization is incorporated into the OCBC methods, performance improvements are observed across all tasks, albeit to varying degrees. This enhancement is attributed to the fact that **GCREinSL** allows for tackling unseen state-goal combination tasks during

the inference phase, thereby improving the generalization and stitching capability of the models. Our **GCR<sub>ein</sub>SL** consistently outperforms the other data augmentation approaches across all Pointmaze tasks, particularly in the more complex Pointmaze-Medium and Pointmaze-Large tasks. The qualitative comparison in Figure 6 indicate that **GCR<sub>ein</sub>SL**, while being SL-based, can effectively address long-horizon tasks that require trajectory stitching similar to the TD-based method IQL.

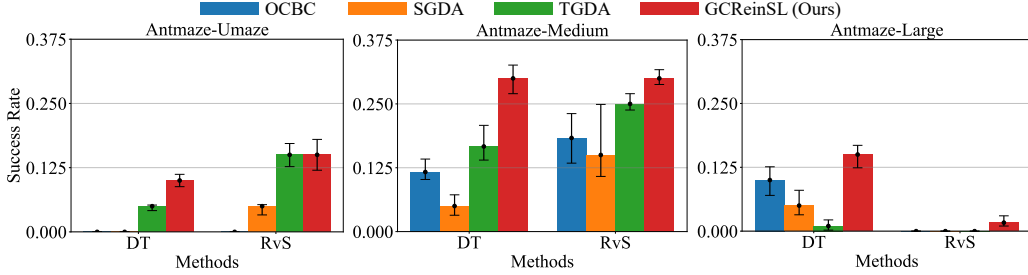


Figure 7: Performance on high-dimensional Ghugare et al. [2024] Antmaze datasets. **GCR<sub>ein</sub>SL** can consistently improve the performance of OCBC and surpass goal data augmentation methods on all high-dimensional Antmaze datasets. Error bars denote 95% bootstrap confidence intervals. We demonstrate that through the learning and utilization of maximum in-distribution  $Q$ -value, **GCR<sub>ein</sub>SL** enhances the stitching capability of OCBC.

### 6.3 Higher-dimensional Datasets Results

To evaluate the performance of our **GCR<sub>ein</sub>SL** to tasks with higher-dimensional input observations, we implemented it on Antmaze and Visual-Pointmaze described in [Ghugare et al., 2024]. In Figure 7, we observe that **GCR<sub>ein</sub>SL** improves the performance of DT and RvS across all Antmaze datasets, with particularly notable improvements on the medium and large datasets. In Appendix G.2, we report the results on Visual-Pointmaze datasets. We find that on all datasets, compared to other data augmentation methods, our **GCR<sub>ein</sub>SL** (almost) always performs better than previous approaches, demonstrating that our method remains effective in the high-dimensional problem setting.

Table 1: The normalized best score on D4RL [Fu et al., 2020] Antmaze-v2 datasets. The results come from its original Reinformer [Zhuang et al., 2024] paper except **GCR<sub>ein</sub>SL**. The best result is **bold** and the blue result means the best result among sequence modeling.

Antmaze-v2	RL (Use TD)		Sequence Modeling (No TD)				
	CQL	IQL	DT	EDT	CGDT	Reinformer	<b>GCR<sub>ein</sub>SL (ours)</b>
umaze	<b>94.8 ± 0.8</b>	84.00 ± 4.1	64.5 ± 2.1	67.8 ± 3.2	71.0	<b>84.4 ± 2.7</b>	80.1 ± 5.3
umaze-diverse	53.8 ± 2.1	<b>79.5 ± 3.4</b>	60.5 ± 2.3	58.3 ± 1.9	<b>71.0</b>	65.8 ± 4.1	67.2 ± 5.3
medium-play	<b>80.5 ± 3.4</b>	78.5 ± 3.8	0.8 ± 0.4	0.0 ± 0.0	/	13.2 ± 6.1	<b>49.0 ± 3.5</b>
medium-diverse	71.0 ± 4.5	<b>83.5 ± 1.8</b>	0.5 ± 0.5	0.0 ± 0.0	/	10.6 ± 6.9	<b>51.7 ± 4.4</b>
large-play	34.8 ± 5.9	<b>53.5 ± 2.5</b>	0.0 ± 0.0	0.6 ± 0.5	/	0.4 ± 0.5	<b>38.2 ± 1.8</b>
large-diverse	36.3 ± 3.3	<b>53.0 ± 3.00</b>	0.0 ± 0.0	0.0 ± 0.0	/	0.4 ± 0.5	<b>30.2 ± 2.4</b>
Total	371.2	432.0	126.3	126.7	/	174.8	<b>316.4</b>

### 6.4 Return-conditioned RL Datasets Results

We also extend our **GCR<sub>ein</sub>SL** to return-conditioned RL (see Appendix B for detailed extensions) and compare it with advanced sequence modeling, as shown in Table 1. From Table 1, it is evident that in the majority of the Antmaze-v2 datasets, particularly in the complex medium and large Antmaze-v2 tasks, the **GCR<sub>ein</sub>SL** approach demonstrates superior performance, significantly bridging the gap with TD-based methods such as CQL. Compared to the two most closely related works EDT [Wu et al., 2023] and Reinformer [Zhuang et al., 2024], we utilize the estimated  $Q$ -value instead of their return-to-go [Chen et al., 2021], which more accurately reflects the quality of actions during the stitching process [Wang et al., 2024b, Kim et al., 2024].

### 6.5 Ablation Study

In this section, we analyze the impact of the hyperparameter  $L$  in the probability estimator (Equation (9)) and  $m$  in the  $Q$ -function loss (Equation (10)). As demonstrated in

the left panel of Figure 8, the performance does not exhibit a linear relationship with increasing values of  $L$ . Therefore, we set  $L = 500$  as the default value for the datasets employed in Ghugare et al. [2024]. For the D4RL Antmaze-v2 datasets [Fu et al., 2020], we select  $L = 5$ , in line with the methodology outlined by Wu et al. [2022]. As outlined in Theorem 5.2, as  $m \rightarrow 1$ , the learned  $Q$ -function asymptotically converges to the maximum  $Q$ -function within the offline distribution. Given that a higher *in-distribution*  $Q$ -function corresponds to improved action selection, we can infer that performance will improve as  $m$  approaches 1. The experimental results presented in the right panel of Figure 8 are consistent with this theoretical prediction. However, larger values of  $m$  do not consistently lead to more effective training or higher performance; in some cases, they may result in a performance decline. This could be attributed to overfitting to excessively large  $Q$ -values present in the offline dataset.

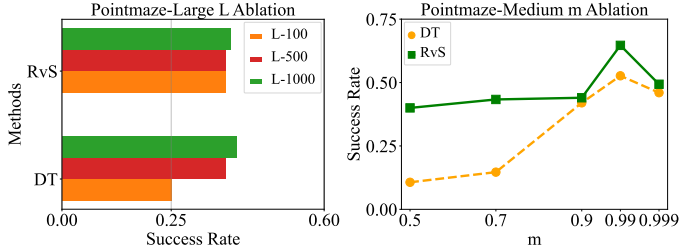


Figure 8: Ablation study of different hyperparameter  $L$  and  $m$  in Ghugare et al. [2024] datasets. **Left:** The performance on the Pointmaze-Large task when applying different values of  $L$  to the importance sampling estimator. **Right:** The trend of last results as  $m$  varies on Pointmaze-Medium task.

## 7 Conclusion

In this work, we introduce a  $Q$ -conditioned maximization supervised learning framework, embedding the maximized  $Q$ -value into SL-based methods (OCBC). To implement this framework, we propose the **GCREinSL** algorithm. Both theoretical analysis and experimental results demonstrate that **GCREinSL** significantly enhances the stitching capability of OCBC as well as sequence modeling methods while maintaining robustness. Future work could focus on developing more advanced OCBC architectures to further bridge the gap with TD learning.

## References

- Rishabh Agarwal, Max Schwarzer, Pablo Samuel Castro, Aaron C Courville, and Marc Bellemare. Deep reinforcement learning at the edge of the statistical precipice. *Advances in neural information processing systems*, 34:29304–29320, 2021.
- Dennis J Aigner, Takeshi Amemiya, and Dale J Poirier. On the estimation of production frontiers: maximum likelihood estimation of the parameters of a discontinuous density function. *International economic review*, pages 377–396, 1976.
- Marcin Andrychowicz, Filip Wolski, Alex Ray, Jonas Schneider, Rachel Fong, Peter Welinder, Bob McGrew, Josh Tobin, OpenAI Pieter Abbeel, and Wojciech Zaremba. Hindsight experience replay. *Advances in neural information processing systems*, 30, 2017.
- Léonard Blier, Corentin Tallec, and Yann Ollivier. Learning successor states and goal-dependent values: A mathematical viewpoint. *arXiv preprint arXiv:2101.07123*, 2021.
- Michał Bortkiewicz, Władysław Pałucki, Vivek Myers, Tadeusz Dziarmaga, Tomasz Arczewski, Łukasz Kuciński, and Benjamin Eysenbach. Accelerating goal-conditioned reinforcement learning algorithms and research. In *The Thirteenth International Conference on Learning Representations*, 2025.
- David Brandfonbrener, Will Whitney, Rajesh Ranganath, and Joan Bruna. Offline rl without off-policy evaluation. *Advances in neural information processing systems*, 34:4933–4946, 2021.
- David Brandfonbrener, Alberto Bietti, Jacob Buckman, Romain Laroche, and Joan Bruna. When does return-conditioned supervised learning work for offline reinforcement learning? *Advances in Neural Information Processing Systems*, 35:1542–1553, 2022.



- Jiahang Cao, Qiang Zhang, Ziqing Wang, Jingkai Sun, Jiaxu Wang, Hao Cheng, Yecheng Shao, Wen Zhao, Gang Han, Yijie Guo, et al. Mamba as decision maker: Exploring multi-scale sequence modeling in offline reinforcement learning. *arXiv preprint arXiv:2406.02013*, 2024.
- Elliot Chane-Sane, Cordelia Schmid, and Ivan Laptev. Goal-conditioned reinforcement learning with imagined subgoals. In *International conference on machine learning*, pages 1430–1440. PMLR, 2021.
- David Cheikhi and Daniel Russo. On the statistical benefits of temporal difference learning. In *International Conference on Machine Learning*, pages 4269–4293. PMLR, 2023.
- Lili Chen, Kevin Lu, Aravind Rajeswaran, Kimin Lee, Aditya Grover, Misha Laskin, Pieter Abbeel, Aravind Srinivas, and Igor Mordatch. Decision transformer: Reinforcement learning via sequence modeling. *Advances in neural information processing systems*, 34:15084–15097, 2021.
- Yiming Ding, Carlos Florensa, Pieter Abbeel, and Mariano Phielipp. Goal-conditioned imitation learning. *Advances in neural information processing systems*, 32, 2019.
- Scott Emmons, Benjamin Eysenbach, Ilya Kostrikov, and Sergey Levine. Rvs: What is essential for offline rl via supervised learning? *arXiv preprint arXiv:2112.10751*, 2021.
- Benjamin Eysenbach, Ruslan Salakhutdinov, and Sergey Levine. C-learning: Learning to achieve goals via recursive classification. *arXiv preprint arXiv:2011.08909*, 2020.
- Benjamin Eysenbach, Soumith Udatha, Russ R Salakhutdinov, and Sergey Levine. Imitating past successes can be very suboptimal. *Advances in Neural Information Processing Systems*, 35: 6047–6059, 2022a.
- Benjamin Eysenbach, Tianjun Zhang, Sergey Levine, and Russ R Salakhutdinov. Contrastive learning as goal-conditioned reinforcement learning. *Advances in Neural Information Processing Systems*, 35:35603–35620, 2022b.
- Benjamin Eysenbach, Vivek Myers, Ruslan Salakhutdinov, and Sergey Levine. Inference via interpolation: Contrastive representations provably enable planning and inference. *Advances in Neural Information Processing Systems*, 37:58901–58928, 2025.
- Justin Fu, Aviral Kumar, Ofir Nachum, George Tucker, and Sergey Levine. D4rl: Datasets for deep data-driven reinforcement learning. *arXiv preprint arXiv:2004.07219*, 2020.
- Scott Fujimoto and Shixiang Shane Gu. A minimalist approach to offline reinforcement learning. *Advances in neural information processing systems*, 34:20132–20145, 2021.
- Dibya Ghosh, Abhishek Gupta, Ashwin Reddy, Justin Fu, Coline Manon Devin, Benjamin Eysenbach, and Sergey Levine. Learning to reach goals via iterated supervised learning. In *International Conference on Learning Representations*, 2021.
- Raj Ghugare, Matthieu Geist, Glen Berseth, and Benjamin Eysenbach. Closing the gap between TD learning and supervised learning - a generalisation point of view. In *The Twelfth International Conference on Learning Representations*, 2024.
- Joey Hejna, Jensen Gao, and Dorsa Sadigh. Distance weighted supervised learning for offline interaction data. *arXiv preprint arXiv:2304.13774*, 2023.
- Mineui Hong, Minjae Kang, and Songhwai Oh. Diffused task-agnostic milestone planner. *Advances in Neural Information Processing Systems*, 36:387–405, 2023.
- Sili Huang, Jifeng Hu, Zhejian Yang, Liwei Yang, Tao Luo, Hechang Chen, Lichao Sun, and Bo Yang. Decision mamba: Reinforcement learning via hybrid selective sequence modeling. *arXiv preprint arXiv:2406.00079*, 2024.
- Vineet Jain and Siamak Ravanbakhsh. Learning to reach goals via diffusion. In *International Conference on Machine Learning*, pages 21170–21195. PMLR, 2024.
- Zhengyao Jiang, Tianjun Zhang, Michael Janner, Yueying Li, Tim Rocktäschel, Edward Grefenstette, and Yuandong Tian. Efficient planning in a compact latent action space. 2023.

- Jeonghye Kim, Suyoung Lee, Woojun Kim, and Youngchul Sung. Adaptive  $q$ -aid for conditional supervised learning in offline reinforcement learning. *Advances in Neural Information Processing Systems*, 37:87104–87135, 2024.
- Junsu Kim, Younggyo Seo, Sungsoo Ahn, Kyunghwan Son, and Jinwoo Shin. Imitating graph-based planning with goal-conditioned policies. *arXiv preprint arXiv:2303.11166*, 2023.
- Diederik Kingma and Jimmy Ba. Adam: A method for stochastic optimization. *Computer Science*, 2014.
- Diederik P Kingma and Max Welling. An introduction to variational autoencoders. *arXiv preprint arXiv:1906.02691*, 2019.
- Ilya Kostrikov, Ashvin Nair, and Sergey Levine. Offline reinforcement learning with implicit  $q$ -learning. *arXiv preprint arXiv:2110.06169*, 2021.
- Aviral Kumar, Justin Fu, Matthew Soh, George Tucker, and Sergey Levine. Stabilizing off-policy  $q$ -learning via bootstrapping error reduction. *Advances in neural information processing systems*, 32, 2019.
- Aviral Kumar, Aurick Zhou, George Tucker, and Sergey Levine. Conservative  $q$ -learning for offline reinforcement learning. *Advances in Neural Information Processing Systems*, 33:1179–1191, 2020.
- Kuang-Huei Lee, Ofir Nachum, Mengjiao Sherry Yang, Lisa Lee, Daniel Freeman, Sergio Guadarrama, Ian Fischer, Winnie Xu, Eric Jang, Henryk Michalewski, et al. Multi-game decision transformers. *Advances in Neural Information Processing Systems*, 35:27921–27936, 2022a.
- Seungjae Lee, Jigang Kim, Inkyu Jang, and H Jin Kim. Dhrl: a graph-based approach for long-horizon and sparse hierarchical reinforcement learning. *Advances in Neural Information Processing Systems*, 35:13668–13678, 2022b.
- Sergey Levine, Aviral Kumar, George Tucker, and Justin Fu. Offline reinforcement learning: Tutorial, review, and perspectives on open problems. *arXiv preprint arXiv:2005.01643*, 2020.
- Jinning Li, Chen Tang, Masayoshi Tomizuka, and Wei Zhan. Hierarchical planning through goal-conditioned offline reinforcement learning. *IEEE Robotics and Automation Letters*, 7(4):10216–10223, 2022.
- Jinxin Liu, Xinghong Guo, Zifeng Zhuang, and Donglin Wang. Didi: diffusion-guided diversity for offline behavioral generation. *arXiv preprint arXiv:2405.14790*, 2024a.
- Jinxin Liu, Ziqi Zhang, Zhenyu Wei, Zifeng Zhuang, Yachen Kang, Sibao Gai, and Donglin Wang. Beyond ood state actions: Supported cross-domain offline reinforcement learning. In *Proceedings of the AAAI Conference on Artificial Intelligence*, volume 38, pages 13945–13953, 2024b.
- Stuart Lloyd. Least squares quantization in pcm. *IEEE transactions on information theory*, 28(2): 129–137, 1982.
- I Loshchilov. Decoupled weight decay regularization. *arXiv preprint arXiv:1711.05101*, 2017.
- Yunhao Luo, Utkarsh A Mishra, Yilun Du, and Danfei Xu. Generative trajectory stitching through diffusion composition. *arXiv preprint arXiv:2503.05153*, 2025.
- Qi Lv, Xiang Deng, Gongwei Chen, Michael Yu Wang, and Liqiang Nie. Decision mamba: A multi-grained state space model with self-evolution regularization for offline rl. *Advances in Neural Information Processing Systems*, 37:22827–22849, 2024.
- Corey Lynch, Mohi Khansari, Ted Xiao, Vikash Kumar, Jonathan Tompson, Sergey Levine, and Pierre Sermanet. Learning latent plans from play. In *Conference on robot learning*, pages 1113–1132. PMLR, 2020.
- Yecheng Jason Ma, Jason Yan, Dinesh Jayaraman, and Osbert Bastani. How far i’ll go: Offline goal-conditioned reinforcement learning via  $f$ -advantage regression. *arXiv preprint arXiv:2206.03023*, 2022.



- Yecheng Jason Ma, Shagun Sodhani, Dinesh Jayaraman, Osbert Bastani, Vikash Kumar, and Amy Zhang. VIP: Towards universal visual reward and representation via value-implicit pre-training. In *The Eleventh International Conference on Learning Representations*, 2023.
- Volodymyr Mnih, Koray Kavukcuoglu, David Silver, Andrei A Rusu, Joel Veness, Marc G Bellemare, Alex Graves, Martin Riedmiller, Andreas K Fidjeland, Georg Ostrovski, et al. Human-level control through deep reinforcement learning. *nature*, 518(7540):529–533, 2015.
- Vivek Myers, Chongyi Zheng, Anca Dragan, Sergey Levine, and Benjamin Eysenbach. Learning temporal distances: Contrastive successor features can provide a metric structure for decision-making. *arXiv preprint arXiv:2406.17098*, 2024.
- Whitney K Newey and James L Powell. Asymmetric least squares estimation and testing. *Econometrica: Journal of the Econometric Society*, pages 819–847, 1987.
- Toshihiro Ota. Decision mamba: Reinforcement learning via sequence modeling with selective state spaces. *arXiv preprint arXiv:2403.19925*, 2024.
- Seohong Park, Dibya Ghosh, Benjamin Eysenbach, and Sergey Levine. Hiql: Offline goal-conditioned rl with latent states as actions. *Advances in Neural Information Processing Systems*, 36:34866–34891, 2023.
- Seohong Park, Tobias Kreiman, and Sergey Levine. Foundation policies with hilbert representations. *arXiv preprint arXiv:2402.15567*, 2024.
- Seohong Park, Kevin Frans, Benjamin Eysenbach, and Sergey Levine. Ogbench: Benchmarking offline goal-conditioned rl. In *International Conference on Learning Representations (ICLR)*, 2025.
- Rafael Figueiredo Prudencio, Marcos ROA Maximo, and Esther Luna Colombini. A survey on offline reinforcement learning: Taxonomy, review, and open problems. *IEEE Transactions on Neural Networks and Learning Systems*, 2023.
- Moritz Reuss, Maximilian Li, Xiaogang Jia, and Rudolf Lioutikov. Goal-conditioned imitation learning using score-based diffusion policies. *arXiv preprint arXiv:2304.02532*, 2023.
- Danilo Jimenez Rezende, Shakir Mohamed, and Daan Wierstra. Stochastic backpropagation and approximate inference in deep generative models. In *ICML*, 2014.
- Tim GJ Rudner, Vitchyr Pong, Rowan McAllister, Yarin Gal, and Sergey Levine. Outcome-driven reinforcement learning via variational inference. *Advances in Neural Information Processing Systems*, 34:13045–13058, 2021.
- Juergen Schmidhuber. Reinforcement learning upside down: Don’t predict rewards – just map them to actions, 2020.
- Dhruv Shah, Benjamin Eysenbach, Nicholas Rhinehart, and Sergey Levine. Rapid exploration for open-world navigation with latent goal models. In *Conference on Robot Learning*, pages 674–684. PMLR, 2022.
- Harshit Sikchi, Rohan Chitnis, Ahmed Touati, Alborz Geramifard, Amy Zhang, and Scott Niekum. Score models for offline goal-conditioned reinforcement learning. In *The Twelfth International Conference on Learning Representations*, 2024.
- Fabian Sobotka and Thomas Kneib. Geoadditive expectile regression. *Computational Statistics & Data Analysis*, 56(4):755–767, 2012.
- Kihyuk Sohn, Honglak Lee, and Xinchen Yan. Learning structured output representation using deep conditional generative models. *Advances in neural information processing systems*, 28, 2015.
- Mark Towers, Jordan K Terry, Ariel Kwiatkowski, JU Balis, Gd Cola, T Deleu, M Goulão, A Kallinteris, A KG, M Krimmel, et al. Gymnasium (mar 2023), 2023.

- Hado Van Hasselt, Yotam Doron, Florian Strub, Matteo Hessel, Nicolas Sonnerat, and Joseph Modayil. Deep reinforcement learning and the deadly triad. *arXiv preprint arXiv:1812.02648*, 2018.
- Ashish Vaswani, Noam Shazeer, Niki Parmar, Jakob Uszkoreit, Llion Jones, Aidan N Gomez, Łukasz Kaiser, and Illia Polosukhin. Attention is all you need. *Advances in neural information processing systems*, 30, 2017.
- Mianchu Wang, Rui Yang, Xi Chen, Hao Sun, Meng Fang, and Giovanni Montana. GOPlan: Goal-conditioned offline reinforcement learning by planning with learned models. *Transactions on Machine Learning Research*, 2024a. ISSN 2835-8856. URL <https://openreview.net/forum?id=zOKAmm8R9B>.
- Tongzhou Wang, Antonio Torralba, Phillip Isola, and Amy Zhang. Optimal goal-reaching reinforcement learning via quasimetric learning. In *International Conference on Machine Learning*, pages 36411–36430. PMLR, 2023.
- Yuanfu Wang, Chao Yang, Ying Wen, Yu Liu, and Yu Qiao. Critic-guided decision transformer for offline reinforcement learning. In *Proceedings of the AAAI Conference on Artificial Intelligence*, volume 38, pages 15706–15714, 2024b.
- Jialong Wu, Haixu Wu, Zihan Qiu, Jianmin Wang, and Mingsheng Long. Supported policy optimization for offline reinforcement learning. *Advances in Neural Information Processing Systems*, 35: 31278–31291, 2022.
- Yueh-Hua Wu, Xiaolong Wang, and Masashi Hamaya. Elastic decision transformer. *arXiv preprint arXiv:2307.02484*, 2023.
- Taku Yamagata, Ahmed Khalil, and Raul Santos-Rodriguez. Q-learning decision transformer: Leveraging dynamic programming for conditional sequence modelling in offline rl. In *International Conference on Machine Learning*, pages 38989–39007. PMLR, 2023.
- Rui Yang, Yiming Lu, Wenzhe Li, Hao Sun, Meng Fang, Yali Du, Xiu Li, Lei Han, and Chongjie Zhang. Rethinking goal-conditioned supervised learning and its connection to offline rl. *arXiv preprint arXiv:2202.04478*, 2022.
- Rui Yang, Lin Yong, Xiaoteng Ma, Hao Hu, Chongjie Zhang, and Tong Zhang. What is essential for unseen goal generalization of offline goal-conditioned rl? In *International Conference on Machine Learning*, pages 39543–39571. PMLR, 2023a.
- Wenyan Yang, Huiling Wang, Dingding Cai, Joni Pajarinen, and Joni-Kristen Kämäräinen. Swapped goal-conditioned offline reinforcement learning. *arXiv preprint arXiv:2302.08865*, 2023b.
- Youngsik Yoon, Gangbok Lee, Sungsoo Ahn, and Jungseul Ok. Breadth-first exploration on adaptive grid for reinforcement learning. In *Forty-first International Conference on Machine Learning*, 2024.
- Zilai Zeng, Ce Zhang, Shijie Wang, and Chen Sun. Goal-conditioned predictive coding for offline reinforcement learning. *Advances in Neural Information Processing Systems*, 36:25528–25548, 2023.
- Chongyi Zheng, Benjamin Eysenbach, Homer Walke, Patrick Yin, Kuan Fang, Ruslan Salakhutdinov, and Sergey Levine. Stabilizing contrastive rl: Techniques for offline goal reaching. *arXiv preprint arXiv:2306.03346*, 2023.
- Chongyi Zheng, Ruslan Salakhutdinov, and Benjamin Eysenbach. Contrastive difference predictive coding. In *The Twelfth International Conference on Learning Representations*, 2024.
- Qinqing Zheng, Amy Zhang, and Aditya Grover. Online decision transformer. In *international conference on machine learning*, pages 27042–27059. PMLR, 2022.
- Zifeng Zhuang, Kun Lei, Jinxin Liu, Donglin Wang, and Yilang Guo. Behavior proximal policy optimization. *arXiv preprint arXiv:2302.11312*, 2023.

Zifeng Zhuang, Dengyun Peng, Ziqi Zhang, Donglin Wang, et al. Reinformer: Max-return sequence modeling for offline rl. *arXiv preprint arXiv:2405.08740*, 2024.

Zifeng Zhuang, Dengyun Peng, Donglin Wang, Jiacheng Liu, Xing Lei, Diyu Shi, and Ziqi Zhang. Revisiting the design choices in max-return sequence modeling, 2025.

Brian D Ziebart, Andrew L Maas, J Andrew Bagnell, Anind K Dey, et al. Maximum entropy inverse reinforcement learning. In *Aaai*, volume 8, pages 1433–1438. Chicago, IL, USA, 2008.

## Contents of Appendix

<b>A</b>	<b>Proof of Theorem 5.2</b>	<b>17</b>
<b>B</b>	<b>Extension in Return-conditioned RL</b>	<b>17</b>
<b>C</b>	<b>GCREinSL Implementation Details</b>	<b>18</b>
C.1	Implementation of <b>GCREinSL</b> for DT . . . . .	18
C.2	<b>GCREinSL</b> Algorithm for DT . . . . .	19
C.3	Implementation of <b>GCREinSL</b> for RvS . . . . .	19
C.4	<b>GCREinSL</b> Algorithm for RvS . . . . .	20
<b>D</b>	<b>Baseline Details</b>	<b>20</b>
<b>E</b>	<b>Experiment Details</b>	<b>21</b>
E.1	Offline Datasets . . . . .	21
E.2	Implementation Details . . . . .	22
<b>F</b>	<b>Hyperparameters</b>	<b>23</b>
F.1	Hyperparameter $m$ . . . . .	23
F.2	Context Length $K$ . . . . .	23
<b>G</b>	<b>Additional Results</b>	<b>24</b>
G.1	Average Probability of Improvement . . . . .	24
G.2	Results in Visual Inputs . . . . .	24
G.3	Evaluating the Capability of CVAE to Accurately Estimate Goal-reaching Probability	25
G.4	Training Curves on Goal-conditioned Datasets from Ghugare et al. [2024] . . . . .	27
<b>H</b>	<b>Limitations</b>	<b>28</b>
<b>I</b>	<b>Societal Impact</b>	<b>28</b>

## A Proof of Theorem 5.2

**Theorem A.1.** We first define  $\mathbf{SG} \doteq (s, g, a, Q^\beta)$ . For  $m \in (0, 1)$ , if we denote  $\mathbf{Q}^m(\mathbf{SG}) = \arg \min_{\hat{Q}} \mathcal{L}_{\hat{Q}}^m(\mathbf{SG})$ , then we have

$$\lim_{m \rightarrow 1} \mathbf{Q}^m(\mathbf{SG}) = Q_{\max}, \forall s, g,$$

where  $Q_{\max} = \max_{\mathbf{a} \sim \mathcal{D}} Q^\beta(s, a, g)$  denotes the maximum  $Q$ -value with actions estimated from the offline dataset and  $\mathcal{L}_{\hat{Q}}^m$  is define in Equation (7).

**Proof** The proof primarily relies on the monotonicity property of  $m$ -expectile regression and employs a proof by contradiction.

Firstly, leveraging the monotonicity property of  $m$ -expectile regression [Newey and Powell, 1987], it follows that  $\mathbf{Q}^{m_1} \leq \mathbf{Q}^{m_2}$  for  $0 < m_1 < m_2 < 1$ .

Secondly, for all  $m \in (0, 1)$ , it holds that  $\mathbf{Q}^m \leq Q_{\max}$ . Assume there exists some  $m_3$  such that  $\mathbf{Q}^{m_3} > Q_{\max}$ . In this case, all  $Q$ -values from the offline dataset would satisfy  $Q^\beta < \mathbf{Q}^{m_3}$ . Consequently, the  $Q$ -function loss can be simplified given the same weight  $1 - m_3$ :

$$\begin{aligned} \mathcal{L}_{\mathbf{Q}}^{m_3} &= \mathbb{E} \left[ (1 - m_3) (Q^\beta - \mathbf{Q}^{m_3})^2 \right] \\ &> \mathbb{E} \left[ (1 - m_3) (Q^\beta - Q_{\max})^2 \right]. \end{aligned}$$

This inequality holds because  $Q^\beta \leq Q_{\max} < \mathbf{Q}^{m_3}$ . However, this contradicts the fact that  $\mathbf{Q}^{m_3}$  is derived by minimizing the  $Q$ -function loss. Therefore, the assumption is invalid, and we conclude that  $\mathbf{Q}^m \leq Q_{\max}$  is true. This proof step demonstrates that the predicted  $Q$ -function does not suffer from out-of-distribution (OOD) issues.

Finally, the convergence to this limit is a direct consequence of the properties of bounded and monotonically non-decreasing functions, thereby demonstrating the validity of the theorem.

## B Extension in Return-conditioned RL

To further clarify the differences between DT and our **GCreinSL** in return-conditioned RL, as well as the benefits of these changes, we first provide a comparison of the structure of DT and **GCreinSL** in Figure 9. We can observe that our **GCreinSL** replace the return-to-go (RTG) [Chen et al., 2021] conditioning with the estimated  $Q^\beta$  during policy training, and employs expectile regression loss to obtain the maximized *in-distribution*  $Q$ -value  $Q_{\max}$ . The inference process determines the optimal action  $a^*$  by considering both the given state and model predicted *in-distribution* maximum  $Q$ -value  $Q$ , rather than the *arbitrarily selected* RTG  $RTG_r$  in DT.

The primary benefit of the aforementioned changes stems from the learning of the  $Q$ -function, enabling the agent to obtain higher-quality actions more effectively during the stitching process [Kim et al., 2024]. Additionally, during training, our  $Q^\beta$ -conditioning effectively learns the mapping between the *in-distribution*  $Q$ -value and the corresponding actions in the dataset. In the inference phase, we condition our approach on the maximum  $Q$ -value supported by the dataset, thus eliminating the gap between training and inference while pursuing performance. Unlike DT, which learn the mapping between RTG and action from the dataset during training but selects an *arbitrary* RTG during the inference phase, whose appropriate can be suspicious. In Section 6 we experimentally compare our method and DT, and highlights the importance of an appropriate conditioning  $Q$ -value.

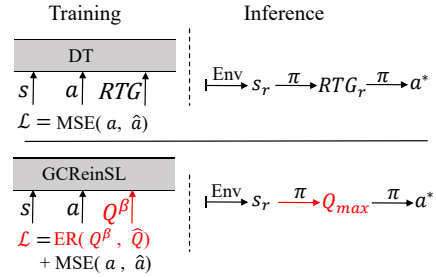


Figure 9: **Left and Right at the Top: DT. Left and Right at the Bottom: GCreinSL.**  $s, a, RTG$  and  $Q^\beta$  are come from offline data  $\mathcal{D}$ .  $s_r$  comes from environment. ER denotes Expectile Regression. The red section highlights the differences.

## C GCREinSL Implementation Details

In this section we focus on the specific implementation of **GCREinSL**, describing the architecture input and output, training, and inference procedures. Specifically, this section describes the training and inference pipeline using typical OCBC algorithm DT. Other supervised learning algorithms can be implemented in a similar manner. The overall structure of **GCREinSL** for DT is depicted in Figure 10, with RvS being similar, differing only in terms of its architecture.

### C.1 Implementation of GCREinSL for DT

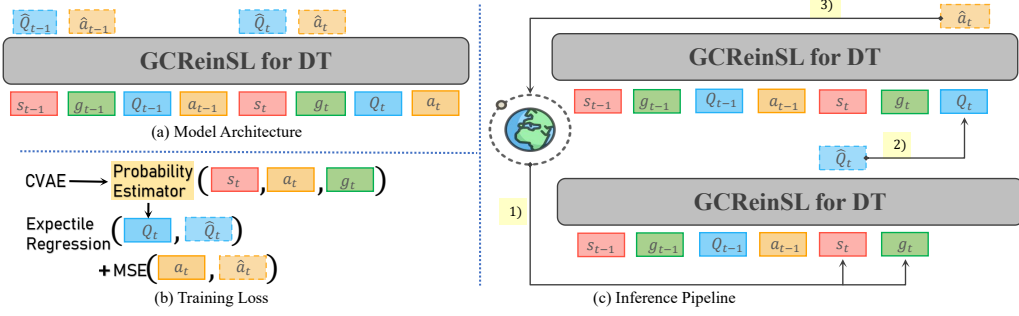


Figure 10: Overview of **GCREinSL** for DT: (a) Model Architecture: The  $Q$ -function is the third inputs of **GCREinSL** for DT and the outputs contain  $Q$ -function and actions. (b) Train Loss: As a  $Q$ -conditioned maximization sequence model, **GCREinSL** for DT not only maximizes the action likelihood but also maximizes  $Q$ -function by expectile regression. (c) Inference Pipeline: When inference, **GCREinSL** for DT first 1) gets state and goal from the environment to predict the *in-distribution* maximum  $Q$ -function. Then 2) predicted *in-distribution* max  $Q$ -function is concatenated with state and goal to predict the optimal action. Finally, 3) the environment executes the predicted action to  $Q$ -function the next state.

**Model Architecture** To accommodate the  $Q$ -conditioned maximization for DT [Chen et al., 2021], which predicts the maximum  $Q$ -value and utilizes it as a condition to guide the generation of optimal actions, we position  $Q$ -value between state and goal. In detail, the input token sequence of **GCREinSL** for DT and corresponding output tokens are summarized as follows:

$$\text{Input: } \langle \dots, s_t^{(n)}, g_t^{(n)}, Q_t^{(n)}, a_t^{(n)} \rangle$$

$$\text{Output: } \langle \hat{Q}_t^{(n)}, \hat{a}_t^{(n)}, \square \rangle$$

$s_t^{(n)}, g_t^{(n)}, Q_t^{(n)}$  and  $a_t^{(n)}$  represent individual tokens within the DT. When predicting the  $\hat{Q}_t^{(n)}$ , the model takes the current state  $s_t^{(n)}$  and previous  $K$  timesteps tokens  $\langle s, g, Q, a \rangle_{t-K}^{(n)} = (s_{t-K+1}^{(n)}, g_{t-K+1}^{(n)}, Q_{t-K+1}^{(n)}, a_{t-K+1}^{(n)}, \dots, s_{t-1}^{(n)}, g_{t-1}^{(n)}, Q_{t-1}^{(n)}, a_{t-1}^{(n)})$  into consideration. For the sake of simplicity,  $\mathbf{SG}_{t-K}^{(n)}$  denotes the input  $[\langle s, g, Q, a \rangle_{t-K}^{(n)}; s_t^{(n)}, g_t^{(n)}]$ . While the action prediction  $\hat{a}_t$  is based on  $(\mathbf{SG}_{t-K}^{(n)}, \mathbf{Q}_{t-K}^{(n)}) = [\langle s, g, Q, a \rangle_{t-K}^{(n)}; s_t^{(n)}, g_t^{(n)}, Q_t^{(n)}]$ . The  $\square$  means that this predicted token neither participates in training nor inference. At timestep  $t$ , different type of tokens are embedded by different linear layers and fed into the transformers [Vaswani et al., 2017] together. The output  $Q$ -function  $\hat{Q}_t^{(n)}$  is processed by a linear layer.

**Training Loss** Since the model predicts both  $\hat{Q}_t$  and  $\hat{a}_t$ , its training loss consists of a  $Q$ -function loss and an action loss. For the action loss, we adopt the MSE loss function of DT and simultaneously adjust the order of tokens:

$$\mathcal{L}_a = \mathbb{E}_{t,n} \left[ a_t^{(n)} - \pi_\theta \left( \mathbf{SG}_{t-K}^{(n)}, \mathbf{Q}_{t-K}^{(n)} \right) \right]^2. \quad (12)$$

The  $Q$ -function loss is the expectile regression with the parameter  $m$ :

$$\mathcal{L}_Q^m = \mathbb{E}_{t,n} [ |m - \mathbb{1}(\Delta Q < 0)| \Delta Q^2 ], \text{ with } \Delta Q = Q_t^{(n)} - \pi_\theta \left( \mathbf{SG}_{t-K}^{(n)} \right). \quad (13)$$

We use the same weight for these two loss functions and therefore the total loss is  $\mathcal{L}_a + \mathcal{L}_Q^m$ .

**Inference Pipeline** For each timestep  $t$ , the action is the last token, which means the predicted action is affected by state from the environment and the  $Q$ -function. The  $Q$ -function of the trajectories output by the sequence model exhibits a positive correlation with the initial conditioned  $Q$ -function [Chen et al., 2021, Zheng et al., 2022]. That is, within a certain range, higher initial  $Q$ -function typically lead to better actions. In classical  $Q$ -learning [Mnih et al., 2015], the optimal value function  $Q^*$  can derive the optimal action  $a^*$  given the current state. In the context of sequence modeling, we also assume that the maximum  $Q$ -value is required to output the optimal actions. The inference pipeline of the **GCREinSL** is summarized as follows:

$$\xrightarrow{\text{Env}} (s_0, g_0) \xrightarrow{\pi_\theta} \hat{Q}_0 \xrightarrow{\pi_\theta} a_0 \xrightarrow{\text{Env}} (s_1, g_1) \xrightarrow{\pi_\theta} \hat{Q}_1 \xrightarrow{\pi_\theta} a_1 \rightarrow \dots \quad (14)$$

Specially, the environment initializes the state-goal pair  $(s_0, g_0)$  and then the sequence model  $\pi_\theta$  predicts the maximum  $Q$ -value  $\hat{Q}_0$  given current state-goal pair  $(s_0, g_0)$ . Concatenating  $\hat{Q}_0$  with  $(s_0, g_0)$ ,  $\pi_\theta$  guarantees the output of the optimal action  $a_0$ . It is important to note that  $(s_0, g_0)$  may be derived from a cross-trajectory. In this case, our  $\pi_\theta$  can still output the optimal action. Then the environment transitions to the next state  $s_1$  and receive the new goal  $g_1$ . Repeat the above steps until the trajectory comes to an end.

## C.2 GCREinSL Algorithm for DT

---

### Algorithm 1 GCREinSL for DT

---

```

1: Input: offline dataset  $\mathcal{D}$ , sequence modeling  $\pi_\theta$ 
2: Initialize VAE with parameters  $\psi$  and  $\varphi$ 
3: Function VAE Training
4:   Sample minibatch of transitions from offline dataset  $\mathcal{D}$ :  $(s, a, g) \sim \mathcal{D}$ 
5:   Update  $\psi, \varphi$  minimizing  $\mathcal{L}_{\text{ELBO}}(s, a, g; \varphi, \psi)$  in Equation (8)
6: //Training Procedure
7: for sample  $\langle \dots, s_t, g_t, a_t \rangle$  from  $\mathcal{D}$  do
8:   Get  $Q_t$  with probability estimator with Equation (9)
9:   Get  $\hat{Q}_t, \hat{a}_t$  with sequence modeling  $\pi_\theta$ :  $\hat{Q}_t, \hat{a}_t = \pi_\theta(\dots, s_t, g_t, a_t, Q_t)$ 
10:  Calculate total loss  $\mathcal{L}_a + \mathcal{L}_Q^m$  by Equation (12) and Equation (13), and take a gradient descent
    step on  $\nabla_\theta (\mathcal{L}_a + \mathcal{L}_Q^m)$ 
11: end for
12: //Inference Pipeline
13: Input: sequence modeling  $\pi_\theta$ , environment Env
14:  $s_0 = \text{Env.reset}()$  and  $t = 0$ 
15: repeat
16:   Predict maximum  $Q$ -function  $\hat{Q}_t = \pi_\theta(\dots, s_t, g_t, \square, \square)$ 
17:   Predict optimal action  $\hat{a}_t = \pi_\theta(\dots, s_t, g_t, \hat{Q}_t, \square)$ 
18:    $s_{t+1}, r_t = \text{Env.step}(\hat{a}_t)$  and  $t = t + 1$ 
19: until done

```

---

## C.3 Implementation of GCREinSL for RvS

**Architecture** To accommodate the  $Q$ -conditioned maximization for RvS [Emmons et al., 2021], which also predicts the maximum  $Q$ -function and utilizes it as a condition to guide the generation of optimal actions. Unlike **GCREinSL** for DT, we construct an actor model for predicting actions and a value model  $v_\phi$  for predicting  $V$ -function. In detail, the input of **GCREinSL** for RvS and

---

In this paper, we do not make a strict distinction between the  $V$ -function and the  $Q$ -function, treating their meanings as equivalent.

corresponding output are summarized as follows:

$$\begin{aligned}
&\textbf{Input: } s_t, g_t, Q_t(s_t, a_t, g_t) \\
&\textbf{Value Model Output: } \hat{V}_t(s_t, g_t) \\
&\textbf{Actor Model Output: } \hat{a}_t(s_t, g_t, \hat{V}_t(s_t, g_t))
\end{aligned}$$

When predicting the  $\hat{V}_t$ , the value model takes the current state  $s_t$  and desired goal  $g_t$ . For action  $\hat{a}_t$ , we adopt a actor model that incorporates  $V$ -values for inference.

**Training Procedure and Inference Pipeline** Like **GCREinSL** for DT, the total loss function is also composed of  $Q$  ( $V$ )-function loss and action loss, and the form is the same. At each step of the inference pipeline, the value model outputs the maximum  $V$ -value for the input state-goal pair, and then the actor model outputs the corresponding action. Note that in this state-goal pair, the state and the goal are treated as distinct elements. In the context of RvS, we also assume that the maximum  $V$ -value are required to output the optimal actions. The training procedure is similar to that of **GCREinSL** for DT, with the key distinction that the prediction of  $V$ -value is generated by a value model. The inference pipeline of the **GCREinSL** is summarized as follows:

$$\stackrel{\text{Env}}{\mapsto} (s_0, g_0) \xrightarrow{v_\phi} \hat{V}_0 \xrightarrow{\pi_\theta} a_0 \stackrel{\text{Env}}{\mapsto} (s_1, g_1) \xrightarrow{v_\phi} \hat{V}_1 \xrightarrow{\pi_\theta} a_1 \rightarrow \dots \quad (15)$$

Specially, the environment initializes the state-goal pair  $(s_0, g_0)$ , and then the value model  $v_\phi$  predicts the maximum  $V$ -value  $\hat{V}_0$  given current state-goal pair. Concatenating  $\hat{V}_0$  with  $(s_0, g_0)$ ,  $\pi_\theta$  can output the optimal action  $a_0$ . Then the environment transitions to the next state  $s_1$  and the desired goal  $g_1$ .

#### C.4 GCREinSL Algorithm for RvS

---

##### Algorithm 2 GCREinSL for RvS

---

```

1: Input: offline dataset  $\mathcal{D}$ , actor model  $\pi_\theta$ , value model  $v_\phi$ 
2: VAE training is similar to GCREinSL for DT.
3: //Training Procedure
4: for sample  $\langle \dots, s_t, g_t, a_t \rangle$  from  $\mathcal{D}$  do
5:   Get  $Q_t$  with probability estimator with Equation (9)
6:   Predict maximum  $V$ -value  $\hat{V}_t = v_\phi(s_t, g_t)$ 
7:   Predict optimal action  $\hat{a}_t = \pi_\theta(s_t, g_t, \hat{V}_t)$ 
8:   The calculation of the total loss is also the same as in GCREinSL for DT.
9: end for
10: //Inference Pipeline
11: Input: value model  $v_\phi$ , actor model  $\pi_\theta$ , environment Env
12:  $s_0 = \text{Env.reset}()$  and  $t = 0$ 
13: repeat
14:   Predict maximum  $V$ -function  $\hat{V}_t = v_\phi(s_t, g_t)$ 
15:   Predict optimal action  $\hat{a}_t = \pi_\theta(s_t, g_t, \hat{V}_t)$ 
16:    $s_{t+1}, r_t = \text{Env.step}(\hat{a}_t)$  and  $t = t + 1$ 
17: until done

```

---

## D Baseline Details

We compare our approach with a wide variety of baselines, including goal data augmentation based stitching methods, sequence modeling and TD-based RL methods.

Particularly, we include the following methods:

- For goal data augmentation methods, we include SGDA [Yang et al., 2023b] and TGDA [Ghugare et al., 2024]. SGDA proposes a method that randomly choose augmented goals from different trajectories. TGDA employs  $k$ -means [Lloyd, 1982] to cluster the goal and



certain states into a group, and samples goals from later stages of these state trajectories as augmented goals. We employ these two goal data augmentation methods in conjunction with DT and RvS as baseline comparisons;

- For sequence modeling methods, we include DT [Chen et al., 2021], EDT [Wu et al., 2023], CGDT [Wang et al., 2024b] and Reinformer [Zhuang et al., 2024]. DT is a classic sequence modeling method that utilizes a Transformer architecture to model and reproduce sequences from demonstrations, integrating a goal-conditioned policy to convert Offline RL into a supervised learning task. Despite its competitive performance in Offline RL tasks, the DT falls short in achieving trajectory stitching [Brandfonbrener et al., 2022]. EDT is a variant of DT that lies in its ability to determine the optimal history length to promote trajectory stitching. But it does not incorporate the RL objective that maximizes returns to enhance the model [Liu et al., 2024a, Zhuang et al., 2024] and its stitching capabilities are limited [Kim et al., 2024]. Reinformer is similar to our work; however, it exhibits limited stitching capabilities due to the absence of  $Q$ -value, resulting in a significant performance gap compared to TD-based RL methods.
- For TD-based RL methods, we include CQL Kumar et al. [2020] and IQL Kostrikov et al. [2021]. CQL and IQL are classical offline RL methods that utilize dynamic programming. This trick endows them with stitching properties [Cheikhi and Russo, 2023, Ghugare et al., 2024].

## E Experiment Details

In this section we provide offline datasets details as well as implementation details used for all the algorithms in our experiments – DT, RvS, CVAE, and **GCREinSL**. Additionally, we report the proportion of computational resources spent on CVAE during the entire **GCREinSL** training process.

### E.1 Offline Datasets

**Goal-conditioned RL** We utilize the Pointmaze, Visual-Pointmaze and Antmaze datasets in Ghugare et al. [2024]. As described in Section 6, both offline datasets contain  $10^6$  transitions and are specifically constructed to evaluate trajectory stitching in a combinatorial setting (see Figure 11). In the Pointmaze dataset, the task involves controlling a ball with two degrees of freedom by applying forces along the Cartesian  $x$  and  $y$  axes. By contrast, the Antmaze dataset features a 3D ant agent, provided by the Farama Foundation [Towers et al., 2023]. The Pointmaze and Visual-Pointmaze were collected using a PID controller, while the Antmaze datasets were generated using a pre-trained policy from D4RL [Fu et al., 2020]. Visual representations of the various Pointmaze configurations can be found in Figure 11.

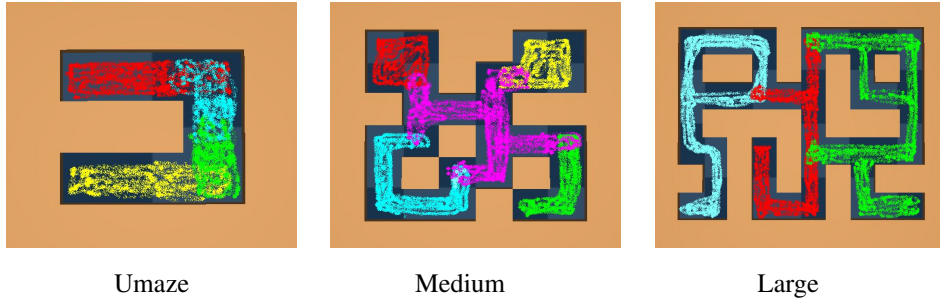


Figure 11: Goal-conditioned RL datasets from Ghugare et al. [2024]: Different colors represent the navigation regions of various data collection policies. During data collection, these policies navigate between randomly selected state-goal pairs within their respective navigation regions. These visualizations pertain to the Pointmaze, with similar patterns observed in the Antmaze datasets.

**Return-conditioned RL** In the experiments comparing with related sequence modeling approaches, we follow the methodology outlined in Zhuang et al. [2024] to construct the AntMaze-v2 datasets using D4RL [Fu et al., 2020], which also contain  $10^6$  transitions (see Figure 12). These AntMaze-v2 datasets are characterized by sparse rewards, where  $r = 1$  is awarded upon reaching the goal. The

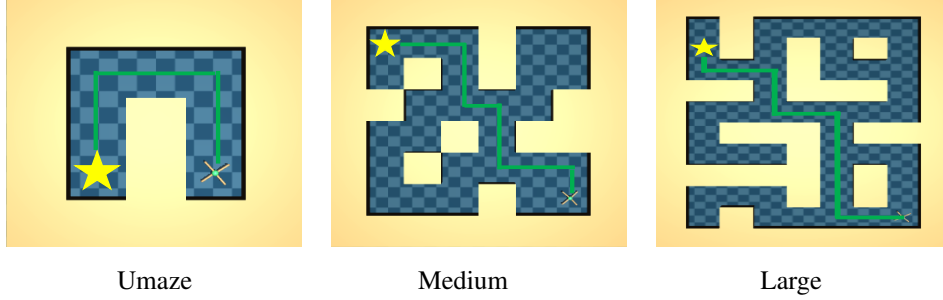


Figure 12: Return-conditioned RL Datasets from Fu et al. [2020]: The AntMaze-v2 datasets involve controlling an 8-DoF quadruped to navigate towards a specified goal state. This benchmark requires value propagation to effectively stitch together sub-optimal trajectories from the collected data.

umaze, medium, and large datasets all lack complete trajectories from the starting point to the desired goal, necessitating that the algorithm reconstructs the desired trajectory by stitching together incomplete or failed segments.

## E.2 Implementation Details

We ran all our experiments on NVIDIA RTX 8000 GPUs with 48GB of memory within an internal cluster. In goal-conditioned RL, we use the default configurations of DT and RvS as described in Ghugare et al. [2024], with some values modified. In goal-conditioned RL, we use the default configurations of DT in Zhuang et al. [2024]. The architecture and training process of the CVAE are identical to those described in SPOT [Wu et al., 2022].

Our **GCREinSL** for DT implementation draws inspiration from and references the following three repositories:

- TGDA: <https://github.com/RajGhugare19/stitching-is-combinatorial-generalisation>;
- SPOT: <https://github.com/thuml/SPOT>;
- Reinformer: <https://github.com/Dragon-Zhuang/Reinformer>.

The state tokens, goal tokens,  $Q$ -function tokens and action tokens are first processed by different linear layers. Then these tokens are fed into the decoder layer to obtain the embedding. Here the decoder layer is a lightweight implementation from Reinformer [Zhuang et al., 2024]. The context length for the decoder layer is denoted as  $K$ . Our **GCREinSL** for RvS implementation is similar to the idea of **GCREinSL** for DT, but it is divided into value networks and policy networks. The value network outputs the expected  $V$ -function from state  $s$  to goal  $g$ . This expected  $V$ -function, along with the state  $s$  and goal  $g$ , is then used as input to the policy network. We employed both the AdamW [Loshchilov, 2017] and Adam [Kingma and Ba, 2014] optimizers to optimize the total loss for DT and RvS, respectively, in alignment with the methods outlined in their original papers. The hyperparameter of  $Q$ -function loss is denoted as  $m$ .

**Practice Implementation of CVAE** Before training the **GCREinSL** algorithm, we first pre-train the CVAE as described in Equation (8). During CVAE training, we sample states and actions from each trajectory in the offline dataset, and we sample future goals from the backend of the same trajectory. In the training process of the **GCREinSL** algorithm, we utilize the importance sampling method outlined in Equation (9) to compute the goal-reaching probability for a given state-goal pair.

**CVAE Computation Cost** The CVAE described in Section 5.3.1 requires only a single training session, after which the  $Q$ -values are inferred in one pass through the density estimator during the training of **GCREinSL**. We evaluated the proportion of computation time consumed by the CVAE-based  $Q$ -function estimation for **GCREinSL** for DT across each dataset, as shown in Table 2. It can be observed that, except for the Antmaze-umaze-v2 and Antmaze-umaze-diverse-v2 datasets, where the CVAE computation time is slightly higher, the proportion of CVAE computation time remains minimal for the other datasets. All train time experiments were run with author-provided implementations on a single RTX 8000 GPU and Intel(R) Xeon(R) Gold 6240 CPU at 2.60GHz.

Table 2: Proportion of CVAE Computation in the Total Training Cost of **GCREinSL**.

Dataset	proportion	Antmaze-umaze-v2	25.6 %
(Visual) Pointmaze-Umaze	(1.52 %) 2.96 %	Antmaze-umaze-diverse-v2	20.83 %
(Visual) Pointmaze-Medium	(1.78 %) 1.61 %	Antmaze-medium-play-v2	9.86 %
(Visual) Pointmaze-Large	(1.44 %) 3.56 %	Antmaze-medium-diverse-v2	7.94 %
Antmaze-Umaze	1.67 %	Antmaze-large-play-v2	9.94 %
Antmaze-Medium (Large)	1.06 % (1.01 %)	Antmaze-large-diverse-v2	8.46 %

## F Hyperparameters

In this section, we will provide a detailed description of parameter settings in our experiments. The hyperparameters of SGDA [Yang et al., 2023b] and TGDA [Ghugare et al., 2024] remain consistent with their original settings. For fair comparison, our method still sets the same **data augmentation probability** of 0.5 as theirs. The default number of training steps is 50000, with a learning rate of 0.001. With these default settings, if the training score continues to rise, we would consider increasing the number of training steps or doubling the learning rate. For some datasets, 50000 steps may cause overfitting and less training steps are better. The hyperparameters of **GCREinSL** for DT in various datasets are presented in the tables below. In all tables, the arrows indicate the directional change in the corresponding values for RvS.

### F.1 Hyperparameter $m$

The hyperparameter  $m$  is crucially related to the  $Q$ -function loss and is one of our primary focuses for tuning. We explore values within the range of  $m = [0.7, 0.9, 0.99, 0.999]$ . When  $m = 0.5$ , the expectile loss function will degenerate into MSE loss, which means the model is unable to output a maximized  $Q$ -function. So we do not take  $m = 0.5$  into consideration. We observe that performance is generally lower at  $m = 0.9$  compared to others except Pointmaze-Umaze. Only Pointmaze-Large adopt the parameter  $m = 0.999$  while  $m = 0.99$  are generally better than  $m = 0.999$  on other datasets. The detailed hyperparameter selection of  $m$  is summarized in the following Table 3:

Table 3: Hyperparameters  $m$  of  $Q$ -function loss on different datasets.

Dataset	$m$	Antmaze-umaze-v2	0.9
(Visual) Pointmaze-Umaze	(0.9) 0.9 $\rightarrow$ 0.99	Antmaze-umaze-diverse-v2	0.99
(Visual) Pointmaze-Medium	(0.99) 0.99	Antmaze-medium-play-v2	0.99
(Visual) Pointmaze-Large	(0.9 $\rightarrow$ 0.99) 0.99 $\rightarrow$ 0.999	Antmaze-medium-diverse-v2	0.99
Antmaze-Umaze	0.99	Antmaze-large-play-v2	0.99
Antmaze-Medium/Large	0.99	Antmaze-large-diverse-v2	0.99

### F.2 Context Length $K$

The context length  $K$  is another key hyperparameter in **GCREinSL** for DT, and we conduct a parameter search across the values  $K = [2, 5, 10, 20]$ . The maximum value is 20 because the default context length for DT [Chen et al., 2021] is 20. The minimum is 2, which corresponds to the shortest sequence length (setting  $K = 1$  would no longer constitute sequence learning). Overall, we found that  $K = 10$  and  $K = 20$  lead to more stable learning and better performance on Ghugare et al. [2024] Pointmaze and Antmaze datasets. Conversely, a smaller context length is preferable on D4RL Antmaze-v2 dataset. The parameter  $K$  has been summarized as follow Table 4:

Table 4: Context length  $K$  on different datasets.

Dataset	$K$	Antmaze-umaze-v2	2
(Visual) Pointmaze-Umaze	(10) 10	Antmaze-umaze-diverse-v2	2
(Visual) Pointmaze-Medium	(20) 10	Antmaze-medium-play-v2	3
(Visual) Pointmaze-Large	(10) 5	Antmaze-medium-diverse-v2	2
Antmaze-Umaze	20	Antmaze-large-play-v2	3
Antmaze-Medium/Large	20	Antmaze-large-diverse-v2	2

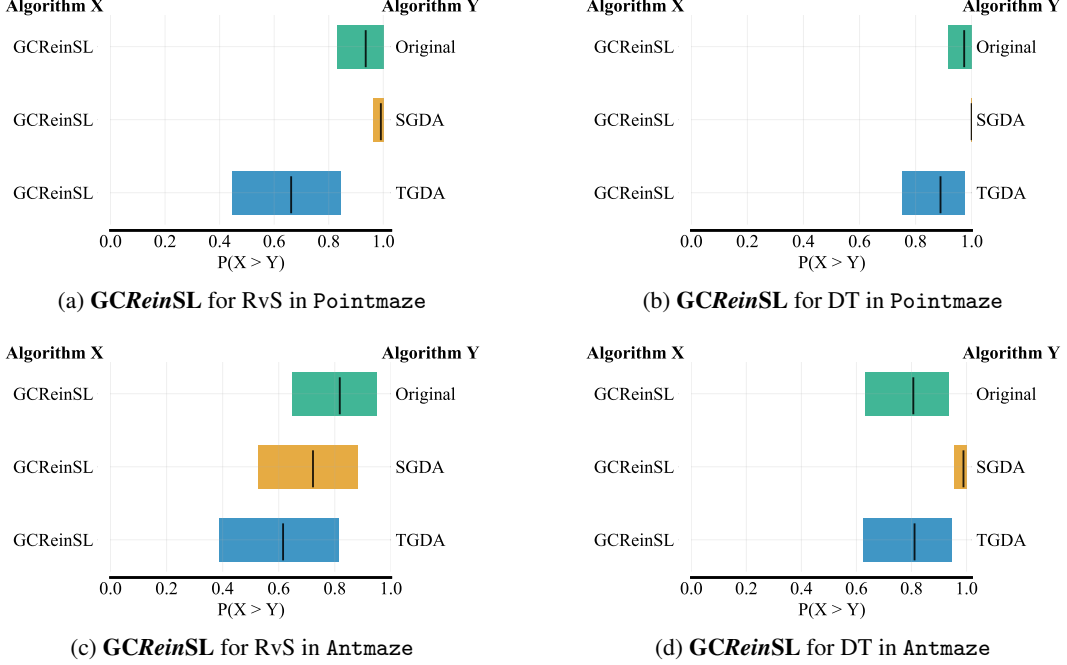


Figure 13: Average probability of improvement on offline (a) (b) Pointmaze and (c) (d) Antmaze datasets. Each figure shows the probability of improvement of **GCReinSL** compared to original or other data augmentation methods. The interval estimates are based on stratified bootstrap with independent sampling with 2000 bootstrap re-samples.

## G Additional Results

This section evaluates the resilience of **GCReinSL** across several factors, including the average probability of improvement, visual-inputs results, the capability of CVAE to accurately estimate goal probabilities, the qualitative comparison, and training curves on goal-conditioned datasets from Ghugare et al. [2024]. Due to space constraints, not all of these variations are discussed in the main body of this study. The details are provided below.

### G.1 Average Probability of Improvement

In this subsection, we adopt the average probability of improvement [Agarwal et al., 2021], a robust metric to measure how likely it is for one algorithm to outperform another on a randomly selected task. The results are reported in Figure 13. As shown in the results, **GCReinSL** robustly outperforms other data augmentation baselines on the Pointmaze datasets. For instance, **GCReinSL** for DT is 98% better than original DT method and 100% better than SGDA. On the complex Antmaze datasets, the probability trend of outperforming the baselines is consistent, whether for **GCReinSL** for DT or **GCReinSL** for RvS. Note that the most two effective and robust algorithms on both Pointmaze and Antmaze datasets are **GCReinSL** and TGDA, which are specifically designed for trajectory stitching. Comparing the two algorithms, **GCReinSL** outperforms TGDA with an average probability of 77.5% on the Pointmaze datasets and 62% on the Antmaze datasets.

### G.2 Results in Visual Inputs

As shown in Figure 14, the comparison between **GCReinSL** and OCBC, related state-of-the-art goal data augmentation methods in the Visual-Pointmaze dataset, demonstrates its scalability to visual observations. **GCReinSL** enhances the stitching performance of OCBC methods across all tasks, highlighting the strength of SL methods in datasets with diverse state-goal distributions. It is noteworthy that SGDA exhibits the lowest robustness, performing even worse than the original DT on the Visual-Pointmaze-Medium and Visual-Pointmaze-Large dataset. This suggests that

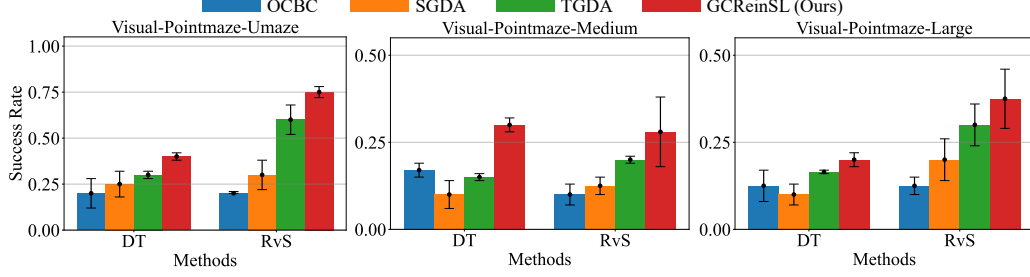


Figure 14: Performance of the original OCBC, as well as OCBC with corresponding goal data augmentation, compared to our SL method on the Visual-Pointmaze datasets from Ghugare et al. [2024]. We use the final mean success rate as the report. Error bars denote 95% bootstrap confidence intervals. **GCReinSL** not only improves the performance of DT and RvS in all tasks, but also outperforms existing goal data augmentation methods.

the random selection of goals may result in the inclusion of numerous low-quality goals, such as unreachable goals [Yang et al., 2023b].

### G.3 Evaluating the Capability of CVAE to Accurately Estimate Goal-reaching Probability

In this section, we validate the accuracy of the CVAE’s estimation of the discounted future state distribution by implementing the computation method outlined in Eysenbach et al. [2020] within a tabular setting. It is important to note that here we are solely validating the accuracy of the CVAE in estimating the discounted future state distribution, which is unrelated to the actual implementation of the CVAE in our **GCReinSL** framework.

Specifically, we compute the true discounted future state distribution in a modified GridWorld environment example and evaluate the estimation error by comparing it against the true distribution. We also compare the predictions of  $Q$ -learning and C-learning [Eysenbach et al., 2020] with the true future state density. First, we introduce the modified GridWorld environment used in this experiment. This environment is characterized by stochastic dynamics and a continuous state space, such that the true  $Q$ -function for the indicator reward is zero. Specifically, the environment has a size of  $5 \times 5$ , where the agent observes a noisy version of its current state. More precisely, when the agent is located at position  $(i, j)$ , it observes the state  $(i + \epsilon_i, j + \epsilon_j)$ , where  $\epsilon_i, \epsilon_j \sim \text{Unif}[-0.5, 0.5]$ . Note that the observation uniquely identifies the agent’s position, so there is no partial observability. Similar to Eysenbach et al. [2020], we analytically compute the exact future state density function by first determining the future state density of the underlying GridWorld, noting that the density is uniform within each cell. We generated a tabular policy by sampling from a Dirichlet (1) distribution, and sampled 100 trajectories of length 100 from this policy for CVAE training.



Figure 15: **Experiments on the effectiveness of density estimation using CVAE.** **Left:** We evaluate CVAE, C-learning, and  $Q$ -learning for predicting the future state distribution in the on-policy setting. As anticipated, CVAE and C-learning achieves lower errors than  $Q$ -learning. On the other hand, CVAE and MC C-learning exhibit comparable performance. **Middle:** and **Right:** The visual comparison. For a given state, action, and future goal in the GridWorld trajectory data, we visualize the comparison between the actual future state density (goal-reaching probability) and the estimates provided by the CVAE. The results indicate a minimal difference, further validating the effectiveness of the CVAE in estimating the future state density (goal-reaching probability).

**Analytic Future State Distribution** Then, as described in Eysenbach et al. [2020], we can compute the true discounted future state distribution by first constructing the following two metrics:

$$T \in \mathbb{R}^{25 \times 25} : T[s, s'] = \sum_a \mathbb{1}(f(s, a) = s') \pi(a | s)$$

$$T_0 \in \mathbb{R}^{25 \times 4 \times 25} : T[s, a, s'] = \mathbb{1}(f(s, a) = s'),$$

where  $f(s, a)$  denotes the deterministic transition function. The future discounted state distribution is then given by:

$$\begin{aligned} P &= (1 - \gamma) [T_0 + \gamma T_0 T + \gamma^2 T_0 T^2 + \gamma^3 T_0 T^3 + \dots] \\ &= (1 - \gamma) T_0 [I + \gamma T + \gamma^2 T^2 + \gamma^3 T^3 + \dots] \\ &= (1 - \gamma) T_0 (I - \gamma T)^{-1} \end{aligned}$$

The tensor-matrix product  $T_0 T$  is equivalent to `einsum('ijk,kh → ijh', T_0, T)`. We use the forward KL divergence for estimating the error in our estimate,  $D_{\text{KL}}(P || Q)$ , where  $Q$  is the tensor of predictions:

$$Q \in \mathbb{R}^{25 \times 4 \times 25} : Q[s, a, g] = q(g | s, a).$$

Following the configuration outlined in Eysenbach et al. [2020], we compare the accuracy of the future discounted state distribution under against C-Learning and  $Q$ -learning:

**On-policy Setting** Figure 15 presents the results of our evaluation comparing CVAE, C-learning, and  $Q$ -learning on the above modified "continuous GridWorld" environment under the on-policy setting. In this scenario, CVAE and C-learning demonstrates lower error compared to  $Q$ -learning, while CVAE achieves the same performance with Monte Carlo C-learning. This highlights the accuracy of CVAE in estimating the discounted state occupancy measure. This experiment aims to answer whether C-learning,  $Q$ -learning and CVAE solve the future state density estimation problem (Equation (1)).

#### G.4 Training Curves on Goal-conditioned Datasets from Ghugare et al. [2024]

The training curves for nine datasets from Ghugare et al. [2024] are shown in Figure 16. The training process for Pointmaze-Umaze exhibits relatively stable behavior. However, the training on Pointmaze-Medium and Pointmaze-Large is characterized by high variance and significant fluctuations. Similarly, the Antmaze-Umaze dataset exhibits some degree of instability. Additionally, the performance on this dataset is notably poor. In contrast, performance on the Antmaze-Medium dataset shows a stable improvement, with the trends for **GCREinSL** for DT and **GCREinSL** for RvS aligning closely. On the Antmaze-Large dataset, the majority of average success rates are near zero.

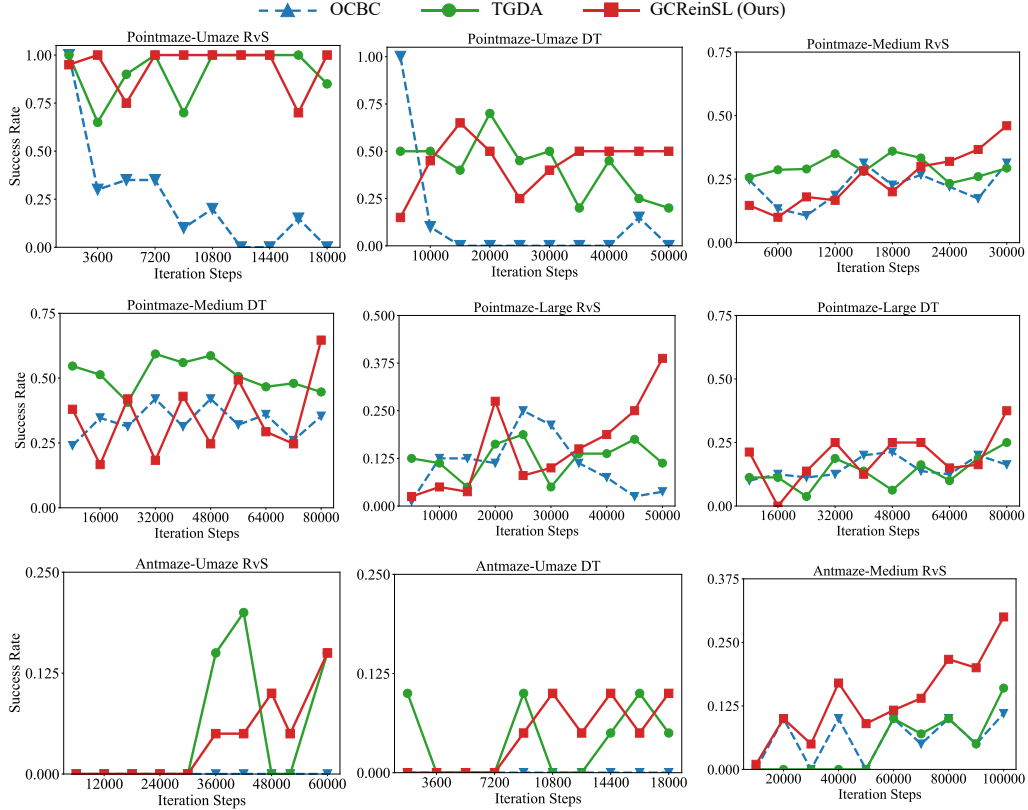


Figure 16: Training curves of OCBC and related goal data augmentation methods on Ghugare et al. [2024] datasets. Although our **GCREinSL** method exhibits some instability on certain datasets, on average, **GCREinSL** tends to improve and achieves promising results with extended training. A potential direction for future research is to develop a more robust **GCREinSL** method that requires less hyperparameter tuning.



## H Limitations

The proposed framework has several limitations. Firstly, the CVAE might pose errors in the estimation of the discounted state occupancy distribution, which will subsequently affect the performance of our policy. Ensemble CVAE is a potential mitigation solution.

Secondly, while SL methods, such as sequence modeling, are straightforward and efficient, their actual performance still falls short compared to classical RL approaches. Moving forward, it is essential to develop more advanced SL methods that not only surpass the performance of traditional RL techniques but also fully exploit the advantages inherent in SL. For example, by integrating our  $Q$ -conditioned maximization with Decision Mamba [Lv et al., 2024, Ota, 2024, Huang et al., 2024, Cao et al., 2024, Zhuang et al., 2025].

## I Societal Impact

This paper presents research aimed at advancing the field of RL. This research is centered on enhancing the stitching capability in the field of offline reinforcement learning: OCBC methods. By overcoming their limitations, it contributes to the advancement of offline reinforcement learning. As foundational research in machine learning, this study does not lead to negative societal outcomes.